Signal Processing by Generalized Receiver in DS-CDMA Wireless Communication Systems with Frequency-Selective Channels

Vyacheslav Tuzlukov

Circuits, Systems, and Signal Processing

ISSN 0278-081X
Volume 30
Number 6

Circuits Syst Signal Process (2011)
30:1197-1230
DOI 10.1007/s00034-011-9273-1

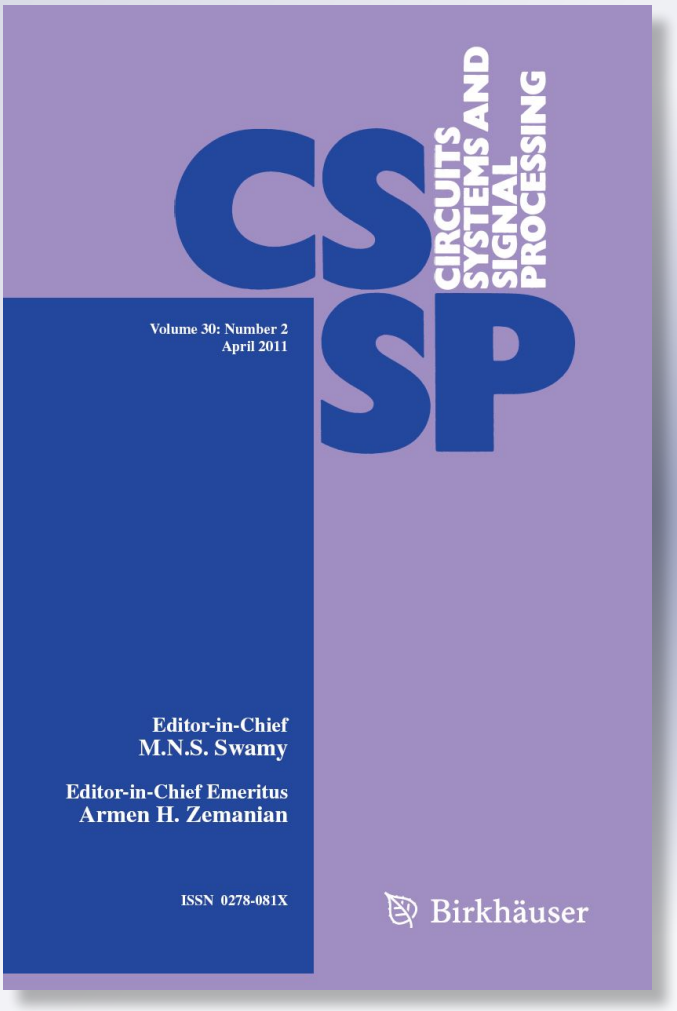

Springer

Circuits Syst Signal Process (2011) 30:1197–1230
DOI 10.1007/s00034-011-9273-1

Signal Processing by Generalized Receiver in DS-CDMA Wireless Communication Systems with Frequency-Selective Channels

Vyacheslav Tuzlukov

Received: 15 November 2009 / Revised: 26 July 2010 / Published online: 2 February 2011

Abstract The generalized receiver (GR) based on a generalized approach to signal processing (GASP) in noise is investigated in a direct-sequence code-division multiple access (DS-CDMA) wireless communication system with frequency-selective channels. We consider four avenues: linear equalization with finite impulse response (FIR) beamforming filters; channel estimation and spatially correlation; optimal combining; and partial cancellation. We investigate the GR with simple linear equalization and FIR beamforming filters. Numerical results and simulation show that the GR with FIR beamforming filters surpasses in performance the optimum infinite impulse response beamforming filters with conventional receivers, and can closely approach the performance of GR with infinite impulse response beamforming filters. Channel estimation errors are taken into consideration so that DS-CDMA wireless communication system performance will not be degraded under practical channel estimation. GR takes an estimation error of a maximum likelihood (ML) multiple-input multiple-output (MIMO) channel estimation and GR spatially correlation into account in computation of minimum mean square error (MMSE) and log-likelihood ratio (LLR) of each coded bit. The symbol error rate (SER) performance of DS-CDMA employing GR with a quadrature sub-branch hybrid selection/maximal-ratio combining (HS/MRC) scheme for 1-D modulations in Rayleigh fading is obtained and compared with that of conventional HS/MRC receivers. Procedure of selecting a partial cancelation factor (PCF) for the first stage of a hard-decision partial parallel interference cancellation (PPIC) of the GR employed in DS-CDMA wireless communication system is proposed. A range of optimal PCFs is derived based on the Price's theorem. Computer simulation results show superiority in bit error rate (BER) performance that is very close to that potentially achieved and surpasses the BER performance of the real PCF for DS-CDMA systems discussed in literature.

V. Tuzlukov (✉)
Department of Communications and Information Engineering, School of Electronics Engineering, College of IT Engineering, Kyungpook National University, 1370 Sankyuk-dong, Buk-gu, Daegu 702-701, South Korea
e-mail: Tuzlukov@ee.knu.ac.kr

Keywords Direct-sequence code-division multiple access (DS-CDMA) · Generalized receiver (GR) · Frequency-selective fading · Signal-to-interference-plus-noise ratio (SINR) · Bit-error rate (BER) performance · Additive white Gaussian noise (AWGN) · Rake receiver · Symbol error rate (SER) performance

1 Introduction

In this paper, we consider and study a generalized receiver (GR) constructed based on a generalized approach to signal processing (GASP) in noise [45–49] and employed in a direct-sequence code-division multiple access (DS-CDMA) wireless communication system with frequency-selective channels. We investigate four avenues: linear equalization with finite impulse response (FIR) beamforming filters; channel estimation and spatially correlation; optimal combining; and partial cancellation.

1.1 Linear Equalization with FIR Beamforming Filters

The use of multiple antennas in wireless communication system attracts significant interest and attention of researchers. Transmit beamforming has received considerable attention because of its simplicity and its ability to exploit the benefits of multiple transmit antennas [11]. Information about channel state at the transmitter is generally required for beamforming. At the present time, the impact of noisy and/or quantized information about the channel state is a pivot of recent research owing to the fact that perfect channel state information may not be available at the transmitter [19, 30, 37]. More recently, in [7], beamforming techniques for systems using a multicarrier approach to cope with frequency-selective fading were also proposed. We should note, however, that the multicarrier techniques are not used in single carrier systems.

In this paper, we investigate the transmit beamforming for single carrier transmission over frequency-selective fading channels with the perfect channel state information at the GR. A necessity of equalization at the GR is generated by the intersymbol interference (ISI) caused by the channel frequency selectivity. It must be emphasized that the optimum beamforming depends on the equalizer used. As is well known, the linear equalization possesses a low complexity. For this reason, we adopt the linear equalization. In comparison and in contrast to [38], we consider the more realistic case of FIR beamforming filters at the GR. Unlike the infinite impulse response case, a closed-form solution for the FIR beamforming filters at the GR does not seem to exist. Because of this, we need to calculate the optimum FIR beamforming filters. Numerical results show that for typical Global System for Mobile Communications/Enhanced Data Rates for GSM Evolution (GSM/EDGE) channels the performance of short GR FIR beamforming filters can be closely approached with infinite impulse response beamforming at the GR and significant gains over single antenna transmission can be achieved.

1.2 Channel Estimation and Spatially Correlation

Under consideration of channel estimation and correlation part, we investigate the minimum mean square error (MMSE) GR. It takes an error of maximum likelihood (ML) multiple-input multiple-output (MIMO) channel estimation and GR spatially correlation into consideration in the computation of MMSE GR and the log-likelihood ratio (LLR) of each coded bit. Our GR analysis and investigation are based on the following statements.

- It is well known [27, 28, 56] that the existing soft-output MMSE vertical Bell Lab Space Time (V-BLAST) detectors have been designed based on perfect channel estimation. Unfortunately, the estimated MIMO channel coefficient matrix is noisy and imperfect in practical application environment [33, 42]. Therefore, these soft-output MMSE V-BLAST detectors will suffer from performance degradation under a practical channel estimation.
- The ML symbol detection scheme is investigated in [42]. It takes into consideration the channel estimation error under the condition that the MIMO channel estimation is imperfect. MMSE based on V-BLAST symbol detection algorithm addressing the impact of the channel estimation error is discussed in [26]. However, the channel coding, decision error propagation compensation, and spatially channel correlation are not discussed and considered.

In the present paper, we derive the MMSE GR for detecting each transmitted symbol and provide the method to compute the LLR of each coded bit. When compared with the detection scheme discussed in [26], our simulation results show that the MMSE GR can obtain sizable performance gain.

1.3 Optimal Combining

In a traditional hybrid selection/maximal-ratio combining (HS/MRC) scheme, the strongest L signals are selected according to the signal-envelope amplitude [3–5, 25, 32, 57, 58]. Optimal maximum likelihood estimation (MLE) of the diversity branch signal phase is implemented by first estimating the in-phase and quadrature branch signal components and obtaining the signal phase as a derived quantity [34, 40]. Other channel estimation procedures also operate by first estimating the in-phase and quadrature branch signal components [1, 43, 44]. Thus, rather than N available signals, there are $2N$ available quadrature branch signal components for combining. In general, the largest $2L$ of these $2N$ quadrature branch signal components will not be the same as the $2L$ quadrature branch signal components of the L branch signals having the largest signal envelopes.

In this paper, we investigate how much improvement in performance can be achieved by using the GR with modified HS/MRC, namely, with quadrature subbranch HS/MRC and HS/MRC schemes, instead of the conventional HS/MRC scheme for 1-D signal modulations in Rayleigh fading. At the GR, the N diversity branches are split into $2N$ in-phase and quadrature subbranches. Then the GR with HS/MRC scheme [21] is applied to these $2N$ subbranches. Obtained results show that the better performance is achieved by this quadrature subbranch HS/MRC scheme in comparison with the traditional HS/MRC one for the same value of average signal-to-noise ratio (SNR) per diversity branch.

1.4 Partial Cancellation

Another problem discussed is the problem of partial interference cancellation. It is well known that the multiple access interference (MAI) can be efficiently estimated by the partial parallel interference cancellation (PPIC) procedure and then be partially canceled out of the received signal on a stage-by-stage basis for a DS-CDMA system [12]. To ensure a good performance, the partial cancellation factor (PCF) for each PPIC stage needs to be chosen appropriately, where the PCF should be increased as the reliability of the MAI estimates improves. In [17, 18, 41], formulas of the optimal PCFs were derived through straightforward analysis based on soft decisions. In contrast, it is very difficult to obtain the optimal PCFs for a detector based on the PPIC with hard decisions owing to their nonlinear character. One common approach to solve the nonlinear problem is to select an arbitrary PCF for the first stage and then increase the value for each successive stage, since the MAI estimates may become more reliable in later stages [12, 15, 59]. This approach is simple, but it might not provide satisfactory performance.

In this paper, we use the Price's theorem [39, 60] to derive a range of the optimal PCF for the first stage in additive white Gaussian noise (AWGN) environment employing the GR, where the lower and upper boundary values of the PCF can be explicitly calculated from the processing gain and the number of users of the DS-CDMA wireless communication system. Computer simulation results show that, using the average of these two boundary values as the PCF for the first stage, we are able to reach the bit error rate (BER) performance that is very close to the potentially achieved one under the use of the GR [22] and surpasses the BER of the real PCF for DS-CDMA wireless communication systems discussed in [40].

With this result, a reasonable PCF can quickly be determined without the use of time-consuming Monte Carlo simulations. It is worth mentioning that the two-stage GR [53] based on the PPIC using the proposed PCF at the first stage achieves the BER performance comparable to that of the three-stage GR based on the PPIC using an arbitrary PCF at the first stage. In other words, under the same BER performance, the proposed approach for selecting the PCF can reduce the complexity of the GR based on the PPIC. Although the PCF selection approach is derived for AWGN environment under employing the GR, it can be applied to multipath fading cases [23, 54].

The paper is organized as follows. In Sect. 2, the problem statement and system model for MIMO system, HS/MRC, synchronous DS-CDMA, and GR are briefly reviewed and discussed. Effects of FIR beamforming for linear equalization at the GR employed by DS-CDMA system is reported in Sect. 3. Section 4 presents an analysis of MMSE GR and computation of LLR. The performance analysis and closed-form derivation of the SER for different types of modulation schemes, such as M-ary PAM, BPSK, QPSK, and M-ary QAM systems is carried out in Sect. 5. Additionally, a great attention is paid to obtain a moment generation function for definition of the SNR per symbol. Section 6 is devoted to determination of PCF taking MAI into account. Section 7 represents simulation results for the considered and discussed four avenues, namely, FIR beamforming; MIMO system and channel estimation; quadrature subbranch HC/MRC GR and conventional HC/MRC GR schemes; and synchronous DS-CDMA system employing GR. Finally, concluding remarks are given in Sect. 8.

2 Problem Statement and System Model

2.1 MIMO System

Consider a MIMO DS-CDMA wireless communication system with N_T transmitting and N_R receiving antennas. The modulated symbols $b[k]$ are taken from a scalar symbol alphabet $\mathcal{F}$ such as quadriphase-shift keying (QPSK) or quadrature amplitude modulation (QAM), and have the following variance:

$$\sigma_b^2 = M\{|b[k]|^2\} = 1, \tag{1}$$

where $E\{\cdot\}$ denotes mathematical expectation. The coefficients of the FIR beamforming filters of length L_g at the transmitting antenna n_t, $1 \le n_t \le N_T$ are denoted by $g_{n_t}[k]$, where $0 \le k \le L_g - 1$ and their energy is normalized to

$$\sum_{n_t=1}^{N_T} \sum_{k=0}^{L_g-1} |g_{n_t}[k]|^2 = 1. \tag{2}$$

The signal transmitted over antenna n_t at time k is given by

$$a_{n_t}[k] = g_{n_t}[k] \otimes b[k], \tag{3}$$

where $\otimes$ denotes a linear discrete-time convolution. The discrete-time received signal at the receiving antenna n_r, $1 \le n_r \le N_R$ can be modeled in the following manner:

$$s_{n_r}[k] = \sum_{n_t=1}^{N_T} h_{n_t n_r}[k] \otimes a_{n_t}[k] + n_{n_r}[k], \tag{4}$$

where $n_{n_r}[k]$ denotes the spatially and temporally AWGN with zero mean and variance given by

$$\sigma_n^2 = M\{|n_{n_r}[k]|^2\} = 0.5N_0, \tag{5}$$

where $0.5N_0$ denotes the two-sided power spectral density of the underlying continuous in time pass-band noise process.

The notation $h_{n_t n_r}[k]$, where $0 \le k \le L - 1$, represents the overall channel impulse response between the transmitting antenna n_t and the receiving antenna n_r of length L. In our model, $h_{n_t n_r}[k]$ contains the combined effects of transmit pulse shaping, wireless channel, receive filtering, and sampling. We assume the existence of a block fading model, i.e., the channel is constant for the duration of at least one data burst before it changes independently to a new realization. In general, $h_{n_t n_r}[k]$ are spatially and temporally correlated because of insufficient antenna spacing and transmit/receive filtering, respectively. Substituting (3) into (4), we obtain

$$s_{n_r}[k] = h_{n_r}^{\text{eq}}[k] \otimes b[k] + n_{n_r}[k], \tag{6}$$

where the equivalent channel impulse response $h_{n_r}^{\mathrm{eq}}[k]$ corresponding to the receiving antenna n_r is defined as

$$h_{n_r}^{\mathrm{eq}}[k] = \sum_{n_t=1}^{N_T} h_{n_t n_r}[k] \otimes g_{n_t}[k] \tag{7}$$

and has the length $L_{\mathrm{eq}} = L + L_g - 1$.

Equation (6) shows that the MIMO system with beamforming can be modeled as an equivalent single-input multiple-output (SIMO) system. Therefore, the GR can use the same equalization, channel estimation, and channel tracking techniques as for a single antenna transmission. In this paper, we assume that the GR employs receive-diversity zero-forcing or MMSE linear equalization [9].

Let us rewrite the main statements and definitions mentioned above in matrix form for our convenience in subsequent analysis of channel estimation. Thus, the received signal can be expressed in the following form:

$$\mathbf{s} = \mathbf{H}\mathbf{a} + \mathbf{n} = \sum_{k=1}^{N_T} \mathbf{h}_k a_k + \mathbf{n}, \tag{8}$$

where $\mathbf{s} = [s_1, s_2, \ldots, s_{N_R}]^T$ is the received signal vector; $\mathbf{H} = [\mathbf{h}_1, \mathbf{h}_2, \ldots, \mathbf{h}_{N_T}]^T$ is the $N_R \times N_T$ MIMO channel coefficient matrix with elements $h_{n_t n_r}[k]$ denoting the channel fading coefficient between the n_tth transmitting antenna and the n_rth receiving antenna.

In this paper, we adopt the following GR spatially correlated MIMO channel model:

$$\mathbf{H} = \sqrt{\mathbf{R_r}}\mathbf{H}_w \tag{9}$$

with $\mathbf{H}_w$ denoting an independent and identically distributed (i.i.d.) matrix with entries obeying the Gaussian law with zero mean and unit variance, and $\mathbf{R_r}$ is $N_R \times N_R$ receive array correlation matrix determined by

$$\mathbf{R_r} = \sqrt{\mathbf{R_r}}\left(\sqrt{\mathbf{R_r}}\right)^H. \tag{10}$$

Then, we have

$$E\left\{\mathbf{H}\mathbf{H}^H\right\} = N_T \mathbf{R_r}. \tag{11}$$

The channel is considered to be flat fading with coherence time of $(N_P + N_D)$ MIMO vector symbols, where N_P symbol intervals are dedicated to pilot matrix $\mathbf{S}_p$ and the remaining N_D to data transmission. $\mathbf{a} = [a_1, a_2, \ldots, a_{N_T}]^T$ is the transmitted complex signal vector whose element given by (3) is taken from the complex modulation constellation $\mathcal{F}$, because the modulated symbols $b[k]$ are taken from the scalar symbol alphabet $\mathcal{F}$, such as the QPSK signal, by mapping the coefficient of FIR beamforming filters $g_{n_t}[k]$ like the coded bit vector

$$\mathbf{g}_{n_t} = \left[\mathbf{g}_{n_t}^1, \mathbf{g}_{n_t}^2, \ldots, \mathbf{g}_{n_t}^{\log_2 M}\right]^T \tag{12}$$

to one modulation symbol belonging to $\mathcal{F}$, i.e., $a_{n_t} = \mathrm{map}(\mathbf{g}_{n_t}) \in \mathcal{F}$.

Meanwhile, we assume that each transmitted symbol is independently taken from the same modulation constellation $\mathcal{F}$ and has the same average energy, i.e.,

$$E\{\mathbf{a}\mathbf{a}^H\} = E_b\mathbf{I}_{N_T}. \tag{13}$$

Finally, $\mathbf{n} = [n_1, n_2, \ldots, n_{N_R}]^T$ is the AWGN vector with covariance matrix determined by

$$\mathbf{K}_\mathbf{n} = E\{\mathbf{n}\mathbf{n}^H\} = \sigma_n^2\mathbf{I}_{N_R}. \tag{14}$$

$\mathbf{I}_{N_T}$ and $\mathbf{I}_{N_R}$ are the identity matrices.

2.2 Hybrid Selection/Maximal-Ratio Combining

We assume that there are N diversity branches experiencing slow and flat Rayleigh fading, and all of the fading processes are i.i.d. During analysis we consider only the hypothesis H_1—"a yes" signal in the input stochastic process. Then the equivalent received baseband signal for the kth diversity branch can be written in the form given by (4) and (6). For our convenience, rewrite the received signal in the following form:

$$\mathbf{s}_k = \mathbf{h}_k a_k + \mathbf{n}_k, \quad k = 1, \ldots, N, \tag{15}$$

where $a_k(t)$, as before, is a 1-D baseband transmitted signal that, without loss of generality, is assumed to be real; $\mathbf{h}_k$ is the channel gain vector for the kth branch subject to Rayleigh fading, and $\mathbf{n}_k(t)$ is a zero-mean AWGN complex vector with two-sided power spectral density $0.5N_0$ with the dimension $\frac{W}{Hz}$.

At the GR front end, for each diversity branch, the received signal is split into its in-phase and quadrature signal components. Then, the conventional HS/MRC scheme is applied over all of these quadrature branches, as presented in Fig. 1. Thus, we can present $\mathbf{h}_k$ and $\mathbf{n}_k$ in the following form: $\mathbf{h}_k = \mathbf{h}_{kI} + j\mathbf{h}_{kQ}$, $\mathbf{n}_k = \mathbf{n}_{kI} + j\mathbf{n}_{kQ}$, where j is the complex value. The in-phase signal component $\mathbf{s}_{kI}$ and quadrature

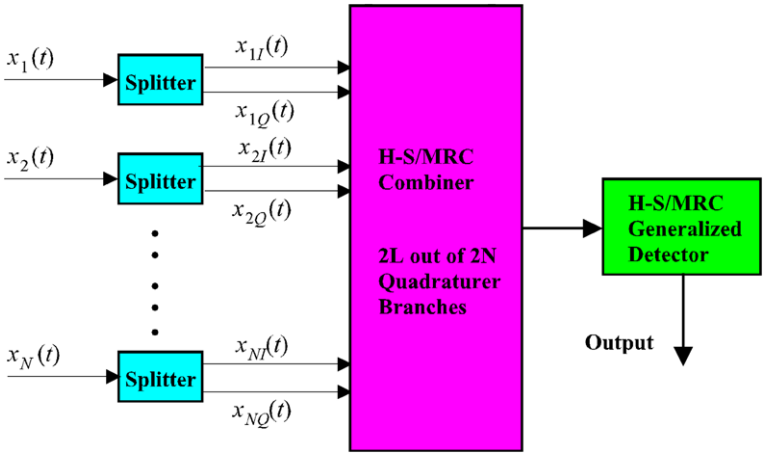

Fig. 1 Block diagram of the GR under quadrature subbranch HS/MRC and HS/MRC schemes

signal component $\mathbf{s}_{kQ}$ of the received signal $\mathbf{s}_k$ are given by $\mathbf{s}_{kI} = \mathbf{h}_{kI}a_k + \mathbf{n}_{kI}$ and $\mathbf{s}_{kQ} = \mathbf{h}_{kQ}a_k + \mathbf{n}_{kQ}$. Since $\mathbf{h}_k$ $(k = 1, \ldots, N)$ are subjected to i.i.d. Rayleigh fading, $\mathbf{h}_{kI}$ and $\mathbf{h}_{kQ}$ are independent zero-mean Gaussian random vectors with the same variance [39],

$$D_h = \frac{1}{2}E\{|\mathbf{h}_k|^2\}. \tag{16}$$

Further, the in-phase $\mathbf{n}_{kI}$ and quadrature $\mathbf{n}_{kQ}$ noise components are also independent zero-mean Gaussian random vectors, each with two-sided power spectral density $0.5N_0$ with the dimension $\frac{W}{Hz}$ [40]. Due to the independence of in-phase $\mathbf{h}_{kI}$ and quadrature $\mathbf{h}_{kQ}$ channel gain components and in-phase $\mathbf{n}_{kI}$ and quadrature $\mathbf{n}_{kQ}$ noise components, the $2N$ quadrature branch received signal components conditioned on the transmitted signal are i.i.d. We can reorganize the in-phase and quadrature components of the channel gains $\mathbf{h}_k$ and Gaussian noise $\mathbf{n}_k$ $(k = 1, \ldots, N)$ as $\mathbf{g}_k$ and $\mathbf{w}_k$, given, respectively, by

$$\begin{aligned} \mathbf{g}_k &= \begin{cases} \mathbf{h}_{kI}, & k = 1, \ldots, N; \\ \mathbf{h}_{(k-N)Q}, & k = N+1, \ldots, 2N; \end{cases} \quad \text{and} \\ \mathbf{w}_k &= \begin{cases} \mathbf{n}_{kI}, & k = 1, \ldots, N; \\ \mathbf{n}_{(k-N)Q}, & k = N+1, \ldots, 2N. \end{cases} \end{aligned} \tag{17}$$

The signal at the output of the GR with quadrature subbranch HS/MRC and HS/MRC schemes takes the following form:

$$\mathbf{Z}^g_{\text{QBHS/MRC}} = \mathbf{s}^2 \sum_{k=1}^{2N} c_k^2 \mathbf{g}_k^2 + \sum_{k=1}^{2N} c_k^2 \mathbf{g}_k^2 \left[\mathbf{w}^2_{k_{\text{AF}}} - \mathbf{w}^2_{k_{\text{PF}}}\right], \tag{18}$$

where $\mathbf{w}^2_{k_{\text{AF}}} - \mathbf{w}^2_{k_{\text{PF}}}$ is the background noise [49] forming at the GR output for the kth branch; $\mathbf{w}^2_{k_{\text{AF}}}$ is the reference complex Gaussian noise with zero mean and finite variance defined below, which is introduced according to GASP [45–49]; $c_k \in \{0, 1\}$ and $2L$ of c_k equal to 1.

2.3 Generalized Receiver (GR)

For better understanding (18), we recall the main functioning principles of GR. The simple model of GR in the form of a block diagram is represented in Fig. 2. In this model, we use the following notation: MSG is the model signal generator (local oscillator), the AF is the additional filter (the linear system) and the PF is the preliminary filter (the linear system). A detailed discussion of the AF and PF can be found in [46] and [47, pp. 233–243 and 264–284]. Consider briefly the main statements regarding the AF and PF.

There are two linear systems at the GR front end that can be presented, for example, as bandpass filters, namely, the PF with the impulse response $h_{\text{PF}}(\tau)$ and the AF with the impulse response $h_{\text{AF}}(\tau)$. For simplicity of analysis, we assume that these filters have the same amplitude-frequency responses and bandwidths. Moreover, a resonant frequency of the AF is detuned relative to a resonant frequency of PF

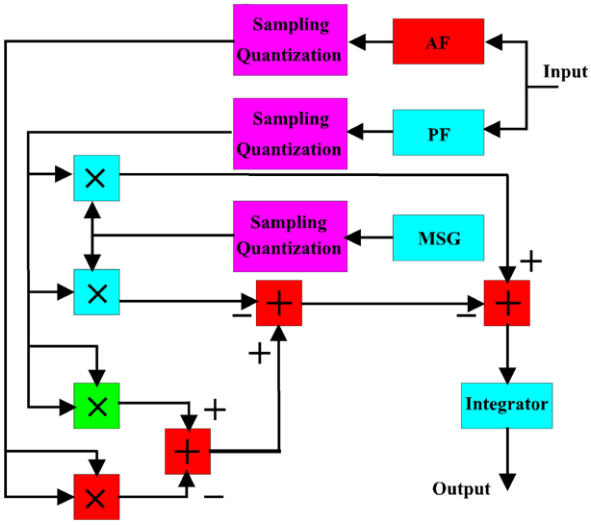

Fig. 2 Principal flowchart model of the GR

on such a value that the signal cannot pass through the AF (with a value that is higher the signal bandwidth). Thus, the signal and noise can appear at the PF output and *the only noise* appears at the AF output. It is well known that if a value of detuning between the AF and PF resonant frequencies is higher than $4–5\Delta f_a$, where Δf_a is the bandwidth of the signal, the processes forming at the AF and PF outputs can be considered as independent and uncorrelated processes (in practice, the coefficient of correlation is not higher than 0.05).

In the case of absence of the signal in the input process, the statistical parameters at the AF and PF outputs will be the same, because the same noise is coming in at the AF and PF inputs, and we may think that the AF and PF do not change the statistical parameters of input process, since they are the linear GR front end systems. For this reason, the AF can be considered as a generator of reference sample with *a priori* information: *a* "*no*" *signal is obtained in the additional reference noise* forming at the AF output.

We need to make some comments regarding the noise forming at the PF and AF outputs. If the Gaussian noise $n(t)$ given by (17) comes in at the AF and PF inputs (the GR linear system front end), the noise forming at the AF and PF outputs is Gaussian, too, because the AF and PF are the linear systems and, in a general case, take the following form:

$$w_{k_{\mathrm{PF}}}(t) = \int_{-\infty}^{\infty} h_{\mathrm{PF}}(\tau) w_k(t-\tau)\, d\tau, \tag{19}$$

and

$$w_{k_{\mathrm{AF}}}(t) = \int_{-\infty}^{\infty} h_{\mathrm{AF}}(\tau) w_k(t-\tau)\, d\tau. \tag{20}$$

If, for example, AWGN with zero mean and two-sided power spectral density $\frac{N_0}{2}$ is coming in at the AF and PF inputs (the GR linear system front end), then the noise

forming at the AF and PF outputs is Gaussian with zero mean and variance given by [47, pp. 264–269]

$$\sigma_n^2 = \frac{N_0\omega_0^2}{8\Delta_F}, \tag{21}$$

where, in the case if the AF (or PF) is the RLC oscillatory circuit, the AF (or PF) bandwidth Δ_F and resonance frequency ω_0 are defined in the following manner:

$$\Delta_F = \pi\beta, \qquad \omega_0 = \frac{1}{\sqrt{LC}}, \quad \text{where } \beta = \frac{R}{2L}. \tag{22}$$

The main functioning condition of GR is the *equality over the whole range of parameters* between the model signal a_k^* forming at the GR MSG output for user k and the expected signal a_k forming at the GR input linear system (the PF) output and additively mixed with noise, i.e.

$$a_k = a_k^*. \tag{23}$$

How we can satisfy this condition in practice is discussed in detail in [46] and [47, pp. 669–695]. More detailed discussion of the choice of PF and AF and their amplitude-frequency responses is also given in [46, 47] (see additionally http://www.sciencedirect.com/science/journal/10512004, click "Volume 8, 1998", "Volume 8, Issue 3", and "A new approach to signal detection theory").

2.4 Synchronous DS-CDMA System

Consider a synchronous DS-CDMA wireless communication system employing the GR with K users and a processing gain N. The received signal can be presented in the following form:

$$\begin{aligned} s(t) &= \sum_{k=1}^{K} A_k h_k b_k d_k(t) + w_{\mathrm{PF}}(t) \\ &= \sum_{k=1}^{K} A_k h_k b_k \sum_{i=1}^{N} d_{ki}\, p_{T_c}(t)(t - iT_c) + w_{\mathrm{PF}}(t), \quad t \in [0, T_b], \end{aligned} \tag{24}$$

where A_k is the transmitted signal amplitude for the kth user; b_k represents the transmitted or modulated bit taking value on ± 1 equiprobably, $\{d_{k1}, d_{k2}, \ldots, d_{kN}\}$ is a random spreading code with each element taking value on $\frac{\pm 1}{\sqrt{N}}$ equiprobably; h_k is the channel fading coefficient; $p_{T_c}(t)$ is the unit-amplitude rectangular pulse with duration T_c; the baseband signal transmitted by the user k is given by $a_k(t) = A_k(t)\sum_{i=1}^{L} b_{k,i} d_k(t - iT_b)$, where $A_k(t)$ is the transmitted signal amplitude of the user k; L is the number of frame;

$$d_k(t) = \sum_{i=1}^{N} d_{ki}\, p_{T_c}(t)(t - iT_c) \tag{25}$$

is the signature waveform of the kth user; $w_{\mathrm{PF}}(t)$ is the zero mean Gaussian noise given by (19); and $T_b = NT_c$ is the bit duration; $S_k(t) = h_k(t)A_k(t)$ is the received signal amplitude envelope for the user k.

Using the GR based on the multistage PPIC for the DS-CDMA wireless communication system and assuming that user l is the desired user, we can express the corresponding output of the GR in accordance with GASP as follows, following faithfully all conditions required for GR functioning [45–49]:

$$Z_l = \int_0^{T_b} 2s_l(t)a^*(t-\tau)\,dt - \int_0^{T_b} s_l(t)s_l(t-\tau)\,dt + \int_0^{T_b} w_{l_{\mathrm{AF}}}(t)w_{l_{\mathrm{AF}}}(t-\tau)\,dt, \tag{26}$$

where $a^*(t-\tau)$ is the model of transmitted signal generated by a local oscillator at the GR receiver given by (23) and τ is the delay factor, which can be neglected for simplicity of analysis.

In this case, we have

$$Z_l = A_l h_l b_l + \sum_{k\neq l}^{K} A_k h_k b_k \rho_{kl} + \zeta_l = A_l h_l b_l + I_l + \zeta_l, \tag{27}$$

where

$$\rho_{kl} = \int_0^{T_b} d_k(t)d_l(t)\,dt \tag{28}$$

is the coefficient of correlation between signature waveforms of the kth and lth users;

$$\zeta_l = \int_0^{T_b} \left[w_{l_{\mathrm{AF}}}^2(t) - w_{l_{\mathrm{PF}}}^2(t)\right] dt \tag{29}$$

is the total noise component at the GR output for the lth user, where $w_{l_{\mathrm{AF}}}^2(t) - w_{l_{\mathrm{PF}}}^2(t)$ is the background noise forming at the output of the universally adopted GR for the lth user [46];

$$I_l = \sum_{k\neq l}^{K} A_k h_k b_k \rho_{kl} \tag{30}$$

is the MAI.

Denoting the soft and hard decisions of the GR output for user l by $\tilde{b}_l^{(0)} = Z_l$ and $\hat{b}_l^{(0)} = \mathrm{sgn}(Z_l)$, respectively, the output of the first PPIC stage with a PCF equal to a_1 can be written [12]

$$\tilde{b}_l^{(1)} = a_1(Z_l - \hat{I}_l) + (1-a_1)\tilde{b}_l^{(0)} = Z_l - a_1\hat{I}_l, \tag{31}$$

where $\tilde{b}_l^{(1)}$ denotes the soft decision of the user l at the first stage of PPIC and

$$\hat{I}_l = \sum_{k\neq l}^{K} A_k \hat{b}_k^{(0)} \rho_{kl} \tag{32}$$

is the estimated MAI using the hard decision.

3 FIR Beamforming for Linear Equalization at the GR

According to [8], the unbiased SNR for linear equalization with the optimum infinite impulse response equalizer filters at the GR back end is given by

$$\mathrm{SNR}(\mathbf{g}) = \frac{\sigma_b^4}{\sigma_e^4} - \chi, \tag{33}$$

where σ_b^2 is given by (1) and the linear equalization error variance σ_e^2 will be defined below. We note that the assumption of infinite impulse response linear equalization filters at the GR back end is not a major restriction, since typically FIR linear equalization filters of length equal to $L_F = 4L_{\mathrm{eq}}$ can approach closely the performance of infinite impulse response linear equalization filters. In (33) we consider the constant $\chi = 0$ for the case of zero-forcing linear equalization and $\chi = 1$ for the case of MMSE linear equalization, respectively [9]. In (33) the beamforming filter vector

$$\mathbf{g} = \big[g_1(0)g_1(1)\cdots g_1(L_g-1)g_2(0)\cdots g_{N_T}(L_g-1)\big]^T \tag{34}$$

consists of the coefficients of all beamforming filters.

The GR linear equalization error variance defined on results discussed in [15] is given by

$$\sigma_e^4 = 4\sigma_n^4 \int_{-0.5}^{0.5} \frac{1}{\sum_{n_r=1}^{N_R} |H_{n_r}^{\mathrm{eq}}(f)|^2 + \mu}\, df, \tag{35}$$

where $\mu = 0$ and $\mu = \frac{4\sigma_n^4}{\sigma_b^4}$ are valid for the case of zero-forcing linear equalization and for the case of MMSE linear equalization, respectively. Furthermore, the frequency response $H_{n_r}^{\mathrm{eq}}(f) = \mathcal{G}\{h_{n_r}^{\mathrm{eq}}(k)\}$ of the equivalent channel can be defined in the following form:

$$H_{n_r}^{\mathrm{eq}}(f) = \mathbf{q}^H(f)\mathbf{H}_{n_r}\mathbf{g}, \tag{36}$$

where the subscript H means the Hermitian transpose,

$$\mathbf{q}(f) = \big\{1 \;\; \exp(j2\pi f) \;\; \cdots \;\; \exp\big[j2\pi f(L_{\mathrm{eq}}-1)\big]\big\}^T, \tag{37}$$

$$\mathbf{H}_{n_r} = \big[\mathbf{H}_{1n_r} \; \mathbf{H}_{2n_r} \; \cdots \; \mathbf{H}_{N_T n_r}\big]^T \tag{38}$$

and $\mathbf{H}_{n_t n_r}$ is a $L_{\mathrm{eq}} \times L_g$ column-circulant matrix with the vector $[h_{n_t n_r}(0) \; \ldots \; h_{n_t n_r}(L-1) \; \mathbf{0}_{L_g-1}^T]^T$ in the first column.

Therefore, the GR SNR with the zero-forcing linear equalization and MMSE linear equalization can be presented in the following form:

$$\mathrm{SNR}(\mathbf{g}) = \frac{\sigma_b^4}{4\sigma_n^4 \int_{-0.5}^{0.5} \frac{1}{\mathbf{g}^H\mathbf{G}(f)\mathbf{g}+\xi}\, df} - \chi \tag{39}$$

with the $N_T L_g \times N_T L_g$ matrix

$$\mathbf{G}(f) = \sum_{n_r=1}^{N_R} \mathbf{H}_{n_r}^H \mathbf{d}(f)\mathbf{d}^H(f)\mathbf{H}_{n_r}. \tag{40}$$

The optimum beamforming filter vector $\mathbf{g}_{\text{opt}}$ shall maximize $\text{SNR}(\mathbf{g})$ subject to the power constraint $\mathbf{g}^H\mathbf{g} = 1$. Unfortunately, this optimization problem is not convex, i.e., the standard tools from convex optimization cannot be applied. Nevertheless, the Lagrangian of the optimization problem can be formulated in the following form:

$$L(\mathbf{g}) = \text{SNR}(\mathbf{g}) + \mu\mathbf{g}^H\mathbf{g}, \tag{41}$$

where μ denotes the Lagrange multiplier.

The optimum vector $\mathbf{g}_{\text{opt}}$ has to satisfy the following equality:

$$\frac{\partial L(\mathbf{g})}{\partial \mathbf{g}^*} = \mathbf{0}_{N_T L_g}, \tag{42}$$

which leads to the nonlinear eigenvalue problem, namely,

$$\left[\int_{-0.5}^{0.5} \frac{\mathbf{G}(f)}{[\mathbf{g}_{\text{opt}}^H\mathbf{G}(f)\mathbf{g}_{\text{opt}} + \xi]^2}\, df\right]\mathbf{g}_{\text{opt}} = \tilde{\mu}\mathbf{g}_{\text{opt}}, \tag{43}$$

with the eigenvalue $\tilde{\mu}$. Unfortunately, (43) does not seem to have a closed-form solution.

Therefore, we use the following gradient algorithm for calculation of the optimum FIR beamforming filters at the GR, which recursively improves an initial beamforming filter vector $\mathbf{g}_0$. The main statements of the gradient algorithm are as follows.

1. Let $i = 0$ and initialized the beamforming filter vector with a suitable $\mathbf{g}_0$ fulfilling $\mathbf{g}_0^H\mathbf{g}_0 = 1$.
2. Update the beamforming filter vector

$$\tilde{\mathbf{g}}_{i+1} = \mathbf{g}_i + \delta\left[\int_{-0.5}^{0.5} \frac{\mathbf{G}(f)}{[\mathbf{g}_i^H\mathbf{G}(f)\mathbf{g}_i + \xi]^2}\, df\right]\mathbf{g}_i, \tag{44}$$

   where δ_i is a suitable adaptation step size.
3. Normalize the beamforming filter vector

$$\mathbf{g}_{i+1} = \frac{\tilde{\mathbf{g}}_{i+1}}{\sqrt{\tilde{\mathbf{g}}_{i+1}^H\tilde{\mathbf{g}}_{i+1}}}. \tag{45}$$

4. If $1 - |\mathbf{g}_{i+1}^H\mathbf{g}_i| < \varepsilon$, go to Step 5, otherwise increment $i \to i+1$ and go to Step 2.
5. $\mathbf{g}_{i+1}$ are the desired beamforming filter vector.

For the termination constant ε in Step 4 a suitably small value should be chosen, e.g. $\varepsilon = 10^{-4}$. Ideally the adaptation step size δ_i should be optimized to maximize

the speed of convergence. Here, we follow [35] and choose δ_i proportional to λ_i^{-1}, where λ_i is the maximal eigenvalue of the matrix

$$\left[\int_{-0.5}^{0.5} \frac{\mathbf{G}(f)}{[\mathbf{g}_i^H \mathbf{G}(f)\mathbf{g}_i + \xi]^2}\, df\right] \tag{46}$$

in iteration i. In particular, we found empirically that $\delta_i = 0.01\lambda_i^{-1}$ is a good choice.

Because of non-convexity of the underlying optimization problem, we cannot guarantee that the gradient algorithm converges to the global maximum. However, adopting the initialization procedure explained below, the solution found by this gradient algorithm seems to be close to optimum, i.e., if L_g is chosen sufficiently large the FIR beamforming filters obtained with the gradient algorithm approach and the performance of the optimal infinite impulse response beamforming filters at the GR was discussed in [53].

We found empirically that a solution with convergence to the optimum or close to optimum is achieved if the beamforming filter length is gradually increased. If the desired beamforming filter length is L_g, the gradient algorithm is executed L_g times. The beamforming filter vector is initialized with the normalized all-ones vector of size N_T for the first execution ($\upsilon = 1$) of the gradient algorithm. For the υth execution, $2 \leq \upsilon \leq L_g$, the first $(\upsilon - 1)$ beamforming filters coefficients of each antenna are initialized with the optimum beamforming filter coefficients for that antenna found in the $(\upsilon - 1)$th execution of the gradient algorithm and the υth coefficients are initialized with zero. In each execution step υ, the algorithm requires typically less than 50 iterations to converge, i.e., the overall complexity of the algorithm is on the order of $50L_g$.

4 MMSE GR

4.1 Channel Estimation

It was proved that for a ML MIMO channel estimator the optimal pilot matrix minimizing the mean square estimation error is an orthogonal pilot matrix [33, 42]. Using the pilot matrix, i.e.,

$$\mathbf{S}_p \mathbf{S}_p^H = E_{\mathrm{P}} N_{\mathrm{P}} \mathbf{I}_{N_T}, \tag{47}$$

where $N_{\mathrm{P}} \geq N_T$ and E_{P} is the energy of each pilot symbol, the estimated channel matrix can be expressed as [33, 42] $\hat{\mathbf{H}} = \mathbf{H} + \Delta\mathbf{H}$, where

$$\Delta\mathbf{H} = \mathbf{n}\mathbf{S}_p^H (E_{\mathrm{P}} N_{\mathrm{P}})^{-1} \tag{48}$$

is the channel estimation error matrix, which is correlated with the matrix $\mathbf{H}$ and with entries subjected to a Gaussian distribution with zero mean and variance

$$\sigma_{\Delta h}^2 = \sigma_n^2 (E_{\mathrm{P}} N_{\mathrm{P}})^{-1}, \tag{49}$$

which is determined independently of instantaneous channel realization. We can conclude that $\hat{\mathbf{H}}$ is a complex Gaussian matrix with zero mean and covariance matrix,

$$\mathrm{Cov}[\hat{\mathbf{H}}] = E\{\hat{\mathbf{H}}\hat{\mathbf{H}}^H\} = N_T(\mathbf{R_r} + \sigma_{\Delta h}^2 \mathbf{I}_{N_R}). \tag{50}$$

Let $\mathbf{h}_m$, $\Delta\mathbf{h}_m$ and $\hat{\mathbf{h}}_m$ $(m = 1, 2, \ldots, N_T)$ denote the mth column of matrices $\mathbf{H}$, $\Delta\mathbf{H}$ and $\hat{\mathbf{H}}$, respectively. Then, by the important properties of complex Gaussian random vector [20] and with some manipulations, we obtain

$$E\{\Delta\mathbf{h}_m|\hat{\mathbf{h}}_m\} = \sigma_{\Delta h}^2 \hat{\mathbf{h}}_m (\mathbf{R_r} + \sigma_{\Delta h}^2 \mathbf{I}_{N_R})^{-1} \tag{51}$$

and

$$\mathrm{Cov}[\Delta\mathbf{h}_m \Delta\mathbf{h}_m^H|\hat{\mathbf{h}}_m] = \sigma_{\Delta h}^2 \mathbf{I}_{N_R} - \frac{\sigma_{\Delta h}^4}{\mathbf{R_r} + \sigma_{\Delta h}^2 \mathbf{I}_{N_R}}. \tag{52}$$

4.2 Computation of MMSE GR

Let $k_i \in \{1, 2, \ldots, N_T\}$ be the index of the ith detected spatial data stream according to the maximal post-detection SINR ordering rule. Denote μ_{a_j} and $\sigma_{a_j}^2$ as the mean and variance of the signal a_j, respectively, which can be determined by a posteriori symbol probability estimation as in [56]. By performing the soft interference cancellation (SIC) [56] and considering the channel estimation error, the corresponding interference-canceled received signal vector $\tilde{\mathbf{s}}_{k_i}$ can be determined in the following form:

$$\begin{aligned}\tilde{\mathbf{s}}_{k_i} &= \mathbf{Ha} - \sum_{j=k_1}^{k_{i-1}} \hat{\mathbf{h}}_j \mu_{a_j} + \mathbf{w}_{\mathrm{PF}} \\ &= \sum_{j=k_i}^{k_{N_T}} (\hat{\mathbf{h}}_j - \Delta\mathbf{h}_j) a_j + \sum_{j=k_1}^{k_{i-1}} \hat{\mathbf{h}}_j (a_j - \mu_{a_j}) - \sum_{j=k_1}^{k_{i-1}} \Delta\mathbf{h}_j a_j + \mathbf{w}_{\mathrm{PF}},\end{aligned} \tag{53}$$

where $\mathbf{w}_{\mathrm{PF}}$ is the noise forming at the PF output of GR front end linear system.

Then, conditionally on $\hat{\mathbf{H}}$, the MMSE GR output is given as [21, 46]

$$\tilde{\mathbf{Y}}_i = \frac{E\{2a_{k_i}\tilde{\mathbf{s}}_{k_i}^H|\hat{\mathbf{H}}\} - E\{\tilde{\mathbf{s}}_{k_i}\tilde{\mathbf{s}}_{k_i}^H|\hat{\mathbf{H}}\} + E\{\mathbf{w}_{\mathrm{AF}_i}\mathbf{w}_{\mathrm{AF}_i}^H\}}{E\{\tilde{\mathbf{s}}_{k_i}\tilde{\mathbf{s}}_{k_i}^H|\hat{\mathbf{H}}\}}, \tag{54}$$

where $\mathbf{w}_{\mathrm{AF}}$ is the reference zero mean Gaussian noise with a priori information: *a "no" signal* and with the following covariance matrix in a general case [46, 47]:

$$E\{\mathbf{w}_{\mathrm{PF}}\mathbf{w}_{\mathrm{PF}}^H\} = E\{\mathbf{w}_{\mathrm{AF}}\mathbf{w}_{\mathrm{AF}}^H\} = \sigma_n^2 \mathbf{I}_{N_R}, \tag{55}$$

because the AF and PF of GR front end linear systems do not change the statistical parameters of input process (Gaussian noise, for example). Thus, according to (53)

and (55), we can write

$$E\{\tilde{\mathbf{s}}_{k_i}\tilde{\mathbf{s}}_{k_i}^H|\hat{\mathbf{H}}\} = \Bigg\{\sum_{j=k_i}^{k_{N_T}}\big[\tilde{\mathbf{h}}_j\tilde{\mathbf{h}}_j^H - \tilde{\mathbf{h}}_j E\{\Delta\mathbf{h}_j^H|\hat{\mathbf{H}}\} - E\{\Delta\mathbf{h}_j|\hat{\mathbf{H}}\}\tilde{\mathbf{h}}_j^H\big] + \sum_{j=1}^{k_{N_T}} E\{\Delta\mathbf{h}_j\Delta\mathbf{h}_j^H|\hat{\mathbf{H}}\}\Bigg\}E_b + \sum_{j=k_1}^{k_{i-1}}\big[\hat{\mathbf{h}}_j\hat{\mathbf{h}}_j^H - \hat{\mathbf{h}}_j E\{\Delta\mathbf{h}_j^H|\hat{\mathbf{H}}\} - E\{\Delta\mathbf{h}_j|\hat{\mathbf{H}}\}\hat{\mathbf{h}}_j^H\big]\sigma_{a_j}^2 + \sigma_n^2\mathbf{I}_{N_R}. \quad (56)$$

Based on results discussed in the previous section, it is evident that $\Delta\mathbf{h}_j$ is only correlated with $\hat{\mathbf{h}}_j$. Then, we have

$$E\{\Delta\mathbf{h}_j\Delta\mathbf{h}_j^H|\hat{\mathbf{H}}\} = E\{\Delta\mathbf{h}_j\Delta\mathbf{h}_j^H|\hat{\mathbf{h}}_j\}. \quad (57)$$

From the basic relationship between the autocorrelation and covariance functions, we have

$$E\{\Delta\mathbf{h}_j\Delta\mathbf{h}_j^H|\hat{\mathbf{h}}_j\} = \mathrm{Cov}\{\Delta\mathbf{h}_j\Delta\mathbf{h}_j^H|\hat{\mathbf{h}}_j\} + E\{\Delta\mathbf{h}_j|\hat{\mathbf{h}}_j\}E\{\Delta\mathbf{h}_j^H|\hat{\mathbf{h}}_j\}. \quad (58)$$

Substituting (51) and (52) into (58), we can write

$$E\{\Delta\mathbf{h}_j\Delta\mathbf{h}_j^H|\hat{\mathbf{h}}_j\} = \sigma_{\Delta h}^2\mathbf{I}_{N_R} - \sigma_{\Delta h}^4\big(\mathbf{R}_\mathbf{r} + \sigma_{\Delta h}^2\mathbf{I}_{N_R}\big)^{-1} + \sigma_{\Delta h}^4\big(\mathbf{R}_\mathbf{r} + \sigma_{\Delta h}^2\mathbf{I}_{N_R}\big)^{-1}\mathbf{h}_j\mathbf{h}_j^H\big(\mathbf{R}_\mathbf{r} + \sigma_{\Delta h}^2\mathbf{I}_{N_R}\big). \quad (59)$$

Introduce the following notation:

$$\mathbf{\Lambda} = \big(\mathbf{R}_\mathbf{r} + \sigma_{\Delta h}^2\mathbf{I}_{N_R}\big)^{-1}, \quad (60)$$

$$\mathbf{\Xi} = \mathbf{I}_{N_R} - \sigma_{\Delta h}^2\Lambda, \quad (61)$$

$$\mathbf{R}_{aa} = \mathrm{diag}\{\sigma_{a_{k_1}}^2, \sigma_{a_{k_2}}^2, \ldots, \sigma_{a_{k_{i-1}}}^2\}. \quad (62)$$

Substituting (51) and (59) into (56) and taking into consideration (60)–(62), we have

$$E\{\tilde{\mathbf{s}}_{k_i}\tilde{\mathbf{s}}_{k_i}^H\} = E_b\mathbf{\Xi}\hat{\mathbf{H}}_{k_i:k_{N_T}}\hat{\mathbf{H}}_{k_i:k_{N_T}}^H\mathbf{\Xi} + E_b\sigma_{\Delta h}^4\mathbf{\Lambda}\hat{\mathbf{H}}_{k_1:k_{i-1}}\hat{\mathbf{H}}_{k_1:k_{i-1}}^H\mathbf{\Lambda} + \big(\hat{\mathbf{H}}_{k_1:k_{i-1}}\mathbf{R}_{aa}\hat{\mathbf{H}}_{k_1:k_{i-1}}^H + N_T E_b\sigma_{\Delta h}^2\big)\mathbf{\Xi} - \sigma_{\Delta h}^2\mathbf{\Lambda}\hat{\mathbf{H}}_{k_1:k_{i-1}}\mathbf{R}_{aa}\hat{\mathbf{H}}_{k_1:k_{i-1}}^H + \sigma_n^2\mathbf{I}_{N_R}, \quad (63)$$

where the notation $\mathbf{H}_{n:m}$ denotes the submatrix containing the nth to mth columns of the matrix $\mathbf{H}$.

Based on similar manipulations, we can write

$$E\{2a_{k_i}\tilde{\mathbf{s}}_{k_i}^H|\hat{\mathbf{H}}\} - E\{\tilde{\mathbf{s}}_{k_i}\tilde{\mathbf{s}}_{k_i}^H|\hat{\mathbf{H}}\} + E\{\mathbf{w}_{\mathrm{AF}_i}\mathbf{w}_{\mathrm{AF}_i}^H\}$$
$$= E_b\hat{\mathbf{h}}_{k_i}^H\sigma_{\Delta h}^2\big(\mathbf{R}_{\mathbf{r}} + \sigma_{\Delta h}^2\mathbf{I}_{N_R}\big)^{-1} + \big(\mathbf{w}_{\mathrm{AF}}\hat{\mathbf{h}}_{k_i}^H\mathbf{w}_{\mathrm{AF}}^H - \mathbf{w}_{\mathrm{PF}}\hat{\mathbf{h}}_{k_i}^H\mathbf{w}_{\mathrm{PF}}^H\big)\mathbf{I}_{N_R}. \quad (64)$$

In the root mean-square sense, the second term in (64) representing the GR back end background noise tends to approach zero. For this reason, finally we can write

$$E\{2a_{k_i}\tilde{\mathbf{s}}_{k_i}^H|\hat{\mathbf{H}}\} - E\{\tilde{\mathbf{s}}_{k_i}\tilde{\mathbf{s}}_{k_i}^H|\hat{\mathbf{H}}\} + E\{\mathbf{w}_{\mathrm{AF}_i}\mathbf{w}_{\mathrm{AF}_i}^H\} = E_b\hat{\mathbf{h}}_{k_i}^H\sigma_{\Delta h}^2\big(\mathbf{R}_{\mathbf{r}} + \sigma_{\Delta h}^2\mathbf{I}_{N_R}\big)^{-1}. \quad (65)$$

Combining (63) and (65), we obtain the MMSE GR $\tilde{\mathbf{Y}}_i$, conditionally on $\hat{\mathbf{H}}$.

4.3 Computation of LLR

By applying $\tilde{\mathbf{Y}}_i$ to $\tilde{\mathbf{s}}_{k_i}$, we have the process at the MMSE GR output [51, 52, 55] $\tilde{Z}_{k_i} = \tilde{\mathbf{Y}}_i\tilde{\mathbf{s}}_{k_i}$. According to the Gaussian approximation of the MMSE GR back end process, we can write

$$\tilde{Z}_{k_i} \approx \tilde{\mu}_{k_i}a_{k_i}^2 + \tilde{\eta}_{k_i}, \quad (66)$$

where

$$\tilde{\mu}_{k_i} = E\{\tilde{\mathbf{Y}}_i(\hat{\mathbf{h}}_{k_i} - \Delta\mathbf{h}_{k_i})|\mathbf{H}\} = \tilde{\mathbf{Y}}_i\Xi\hat{\mathbf{h}}_{k_i} \quad (67)$$

and $\tilde{\eta}_{k_i} = w_{\mathrm{AF}_{ki}}^2 - w_{\mathrm{PF}_{ki}}^2$ is the background noise at the MMSE GR output with zero-mean and variance $\sigma_{\tilde{\eta}_{k_i}}^2 = 4\sigma_n^4$.

Therefore, the LLR value of the coded bit $\mathbf{g}_{k_i}^{\lambda}$ can be approximated as [27, 28]

$$\mathcal{L}\big(\mathbf{g}_{k_i}^{\lambda}\big) \approx \frac{1}{\sigma_{\tilde{\eta}_{k_i}}^2}\Big(\min_{\alpha_i\in\mathcal{F}_{\lambda}^0}|Z_i - \mu_i\alpha_i|^2 - \min_{\alpha_i\in\mathcal{F}_{\lambda}^1}|Z_i - \mu_i\alpha_i|^2\Big), \quad (68)$$

where $\mathcal{F}_{\lambda}^0$ and $\mathcal{F}_{\lambda}^1$ denote the modulation constellation symbols subset of $\mathcal{F}$ whose λth bit equals 0 and 1, respectively.

4.4 Remarks

When the channel estimation error is neglected, i.e., $\sigma_{\Delta h}^2 = 0$ in (60), (61) and (63), the MMSE GR output given by (54) reduces to that of the modified soft-output MMSE GR, in which only decision error propagation is considered [51, 52]. On the other hand, if $\mathbf{R}_{\mathbf{r}} = \mathbf{I}_{N_R}$ and no residual interference cancellation error is assumed, the MMSE GR output given by (54) reduces to that of [55]. For the sake of simplicity, we call this detector the conventional soft-output MMSE GR hereafter if this detector is applied in a channel coded MIMO system. Meanwhile, if both decision error propagation and channel estimation error are neglected, the MMSE GR output given by (54) reduces to that of the conventional MMSE GR output of [24].

5 Performance Analysis

5.1 Symbol Error Rate Expression

Let q_k denote the instantaneous SNR per symbol of the kth quadrature branch ($k = 1, \ldots, 2N$) at the GR back end under the quadrature subbranch HS/MRC and HS/MRC schemes. In line with [47], this instantaneous SNR denoted by q_k can be defined as

$$q_k = \frac{E_b}{\sqrt{4\sigma_n^4}} g_k^2, \tag{69}$$

where E_b is the average symbol energy of the transmitted signal $a_k(t)$. Assume that we choose $2L (1 \le L \le N)$ quadrature branches out of the $2N$ branches. Then, SNR per symbol at the GR back end with the quadrature subbranch HS/MRC and HS/MRC schemes may be presented as $q_{\text{QBHS/MRC}} = \sum_{k=1}^{2L} q_{(k)}$, where $q_{(k)}$ are the ordered instantaneous SNRs q_k and satisfy the following condition: $q_{(1)} \ge q_{(2)} \ge \cdots \ge q_{(2N)}$. When $L = N$, we obtain the MRC, as expected.

Using the moment generating function (MGF) method discussed in [2, 4], the SER of an M-ary pulse amplitude modulation (PAM) system conditioned on $q_{\text{QBHS/MRC}}$ is given by

$$P_{\text{SER}}(q_{\text{QBHS/MRC}}) = \frac{2(M-1)}{M\pi} \int_0^{0.5\pi} \exp\left(-\frac{g_{M\text{-PAM}}}{\sin^2\theta} q_{\text{QBHS/MRC}} \right) d\theta, \tag{70}$$

where $g_{M\text{-PAM}} = 3(M^2 - 1)^{-1}$. Averaging (70) over $q_{\text{QBHS/MRC}}$, the SER of the M-ary PAM system is determined in the following form:

$$\begin{aligned} P_{\text{SER}} &= \frac{2(M-1)}{M\pi} \int_0^{0.5\pi} \int_0^{\infty} \exp\left(-\frac{g_{M\text{-PAM}}}{\sin^2\theta} q \right) f_{q_{\text{QBHS/MRC}}}(q)\, dq\, d\theta \\ &= \frac{2(M-1)}{M\pi} \int_0^{0.5\pi} \varphi_{q_{\text{QBHS/MRC}}} \left(-\frac{g_{M\text{-PAM}}}{\sin^2\theta} \right) d\theta, \end{aligned} \tag{71}$$

where

$$\varphi_q(s) = E_q\{\exp(sq)\} \tag{72}$$

is the MGF of random variable q, $E_q\{\cdot\}$ is the MGF mathematical expectation with respect to SNR per symbol.

When $M = 2$, the average BER performance of a coherent binary phase-shift keying (BPSK) system using the GR with the quadrature subbranch HS/MRC and HS/MRC schemes can be determined in the following form:

$$P_{\text{BER}} = \frac{1}{\pi} \int_0^{0.5\pi} \varphi_{q_{\text{QBHS/MRC}}} \left(-\frac{1}{\sin^2\theta} \right) d\theta. \tag{73}$$

An exact expression for the SER in the case of M-ary PSK system is [10]

$$P_{\text{SER}} = \frac{1}{\pi} \int_0^{\pi - \frac{\pi}{M}} \exp\left\{ -\frac{\frac{E_b}{N_0} \sin^2 \frac{\pi}{M}}{\sin^2\theta} \right\} d\theta. \tag{74}$$

Taking into account (69), (72), and (74), we can write the SER of QPSK system employed the GR in the following form:

$$P_{\mathrm{SER}} = \frac{1}{\pi}\int_0^{\pi-\frac{\pi}{M}} \varphi_{q_{\mathrm{QBHS/MRC}}}\left(-\frac{1}{2\sin^2\theta}\right) d\theta. \tag{75}$$

We need to note that a direct comparison of QPSK and BPSK systems on the basis of average symbol-energy-to-noise-spectral-density ratio indicates that the QPSK is approximately 3 dB worse than the BPSK.

Another signaling scheme that allows multiple signals to be transmitted using quadrature carriers is the QAM. In this case, the transmitted signal can be presented in the following form:

$$a_k(t) = \sqrt{\frac{2}{T_s}}\left[A_i \cos(2\pi f_c t) + B_i \sin(2\pi f_c t)\right], \quad 0 \le t \le T_s, \tag{76}$$

where A_i and B_i take on the possible values $\pm p; \pm 3p, \ldots, \pm(\sqrt{M}-1)p$ with equal probability, where M is an integer power of 4; T_s is the sampling interval, and f_c is the carrier frequency. The parameter p can be related to the average symbol energy E_b as given by

$$p = \sqrt{\frac{3E_b}{2(M-1)}}. \tag{77}$$

Taking into consideration a definition of the SER derived in [61] for M-ary QAM system employed the GR, we obtain

$$\begin{aligned} P_{\mathrm{SER}} = 1 - \frac{1}{M}\Bigg\{ &\left(\sqrt{M}-2\right)^2\left[1 - 2Q\left(\sqrt{\frac{3\varphi_{q_{\mathrm{QBHS/MRC}}}}{M-1}}\right)\right]^2 \\ &+ 4\left(\sqrt{M}-2\right)\left[1 - 2Q\left(\sqrt{\frac{3\varphi_{q_{\mathrm{QBHS/MRC}}}}{M-1}}\right)\right]\left[1 - Q\left(\sqrt{\frac{3\varphi_{q_{\mathrm{QBHS/MRC}}}}{M-1}}\right)\right] \\ &+ 4\left[1 - Q\left(\sqrt{\frac{3\varphi_{q_{\mathrm{QBHS/MRC}}}}{M-1}}\right)\right]^2\Bigg\}, \end{aligned} \tag{78}$$

where $Q(x)$ is the Gaussian Q-function given by

$$Q(x) = \frac{1}{\sqrt{2\pi}}\int_x^\infty \exp\left(-0.5t^2\right) dt. \tag{79}$$

5.2 MGF of $q_{\mathrm{QBHS/MRC}}$

Since all of the $2N$ quadrature branches are i.i.d., the MGF of $q_{\mathrm{QBHS/MRC}}$ takes the following form [5]:

$$\varphi_{q_{\mathrm{QBHS/MRC}}}(s) = 2L\binom{2N}{2L}\int_0^\infty \exp(sq) f(q)\left[\varphi(s,q)\right]^{2L-1}\left[F(q)\right]^{2(N-L)} dq, \tag{80}$$

where $f(q)$ and $F(q)$ are, respectively, the probability density function (pdf) and the cumulative distribution function (cdf) of q of the SNR per symbol for each quadrature branch and

$$\varphi(s,q)=\int_q^\infty \exp(sx)f(x)\,dx \tag{81}$$

is the marginal MGF of the SNR per symbol of a single quadrature branch.

Since g_k and $g_{k+N}(k=1,\ldots,N)$ follow a zero-mean Gaussian distribution with the variance D_h given by (33), one can show that q_k and q_{k+N} follow the Gamma distribution with pdf given by [39]

$$f(q)=\begin{cases}\frac{1}{\sqrt{q}}\exp(-\frac{q}{\bar{q}})\sqrt{\pi\bar{q}}, & q\geq 0,\\ 0, & q\leq 0,\end{cases} \tag{82}$$

where

$$\bar{q}=\frac{2E_bD_h}{\sqrt{4\sigma_n^4}} \tag{83}$$

is the average SNR per symbol for each diversity branch.

Then the marginal MGF on of the SNR per symbol of a single quadrature branch can be determined in the following form:

$$\varphi(s,q)=\frac{1}{\sqrt{1-s\bar{q}}}\operatorname{erfc}\left(\sqrt{\frac{1-s\bar{q}}{\bar{q}}q}\right) \tag{84}$$

and the cdf of q becomes

$$F(q)=1-\varphi(0,q)=1-\operatorname{erfc}\left(\sqrt{\frac{q}{\bar{q}}}\right), \tag{85}$$

where

$$\operatorname{erfc}(x)=\frac{2}{\sqrt{\pi}}\int_x^\infty \exp\left(-t^2\right)dt \tag{86}$$

is the complementary error function.

6 Determination of PCF

In this section, we determine the PCF for the first stage of the PPIC. From [14], the linear MMSE solution of the PCF for the first stage of the PPIC is given by

$$p_{1,\mathrm{opt}}=\frac{\sigma_{2,0}^2-\rho_1\sigma_{1,1}\sigma_{2,0}}{\sigma_{1,1}^2+\sigma_{2,0}^2-2\rho_1\sigma_{1,1}\sigma_{2,0}}, \tag{87}$$

where

$$\sigma_{1,1}^2=E\left\{(I_l+\zeta_l-\hat{I}_l)^2\right\} \tag{88}$$

is the power of the residual MAI plus the background noise forming at the GR back end at the first stage;

$$\sigma_{2,0}^2 = E\{(I_l + \zeta_l)^2\} \tag{89}$$

is the power of the true MAI plus the background noise forming at the GR back end (also called the 0th stage);

$$\rho_1 \sigma_{1,1} \sigma_{2,0} = E\{(I_l + \zeta_l - \hat{I}_l)(I_l + \zeta_l)\} \tag{90}$$

is the correlation between these two interference terms. The linear MMSE solution of the PCF for the first stage of the PPIC can be rewritten as

$$\begin{aligned} p_{1,\mathrm{opt}} &= \frac{E\{(I_l + \zeta_l)\hat{I}_l\}}{E\{\hat{I}_l^2\}} \\ &= \frac{1}{\frac{1}{N}\sum_{u\neq l}^{K} S_u^2 + \sum_{u\neq l}^{K}\sum_{v\neq l,u}^{K} S_u S_v E\{\rho_{ul}\rho_{vl}\hat{b}_u^{(0)}\hat{b}_v^{(0)}\}} \\ &\quad \times \left\{ \frac{1}{N}\sum_{u\neq l}^{K} S_u^2 (1 - 2P_{\mathrm{BER}_{e,u}}) + \sum_{u\neq l}^{K}\sum_{v\neq l,u}^{K} S_u S_v E\{\rho_{ul}\rho_{vl}\hat{b}_u^{(0)}\hat{b}_v^{(0)}\} \right. \\ &\quad \left. + \sum_{v\neq l}^{K} S_v E\{\rho_{vl}\zeta_l \hat{b}_v^{(0)}\} \right\}, \end{aligned} \tag{91}$$

where $S_u(t) = h_u(t)A_u(t)$ is the received signal amplitude envelope for the user u and $A_u(t)$ is the transmitted signal amplitude of user u; $P_{\mathrm{BER}_{e,u}}$ is the BER of user u at the corresponding output of the GR;

$$E\{\hat{b}_u^{(0)}\hat{b}_u^{(0)}\} = 1 - 2P_{\mathrm{BER}_{e,u}} \quad \text{and} \quad E\{\rho_{ul}^2\} = \frac{1}{N}. \tag{92}$$

The channel gain h_u is included into the received signal amplitude envelope $S_u(t)$.

The PCF $p_{1,\mathrm{opt}}$ can be regarded as the normalized correlation between the true MAI plus background noise forming at the GR back end and the estimated MAI. Assume that

$$\mathbf{b} = \{b_k\}_{k=1}^{K} \tag{93}$$

is the data set of all users;

$$\boldsymbol{\rho} = \{\rho_{kl}\}_{k,l=1}^{K} \tag{94}$$

is the correlation coefficient set of random sequences

$$f_{\tilde{b}_v^{(0)}|\mathbf{b},\boldsymbol{\rho}}(\tilde{b}_v^{(0)}|\mathbf{b},\boldsymbol{\rho}) = N\big(E\{\tilde{b}_v^{(0)}|\mathbf{b},\boldsymbol{\rho}\}, 4D_h^2\sigma_n^4\big) \tag{95}$$

is the conditional normal pdf of $\tilde{b}_v^{(0)}$ given $\mathbf{b}$ and $\boldsymbol{\rho}$ and $f_{\tilde{b}_u^{(0)},\tilde{b}_v^{(0)}|\mathbf{b},\boldsymbol{\rho}}(\tilde{b}_u^{(0)},\tilde{b}_v^{(0)}|\mathbf{b},\boldsymbol{\rho})$ is the conditional joint normal pdf of $\tilde{b}_u^{(0)}$ and $\tilde{b}_v^{(0)}$ given $\mathbf{b}$ and $\boldsymbol{\rho}$. Following the

derivations in [12], the expectation terms with hard decisions in (91) can be evaluated based by Price's theorem [39] as follows:

$$E\{\rho_{ul}\rho_{vl}\hat{b}_u^{(0)}\hat{b}_v^{(0)}\} = E\{E\{E\{\rho_{ul}\rho_{vl}\hat{b}_u^{(0)}\hat{b}_v^{(0)}|\mathbf{b},\boldsymbol{\rho}\}|\boldsymbol{\rho}\}\}$$
$$= E\{E\{\rho_{ul}\rho_{vl}\hat{b}_u^{(0)}(2Q_v-1)|\boldsymbol{\rho}\}\}; \tag{96}$$

$$E\{\rho_{vl}\zeta_l\hat{b}_v^{(0)}\} = E\{E\{E\{\rho_{vl}\zeta_l\hat{b}_v^{(0)}|\mathbf{b},\boldsymbol{\rho}\}|\boldsymbol{\rho}\}\}$$
$$= 8D_h^2\sigma_n^4 E\{E\{\rho_{vl}^2 f_{\tilde{b}_v^{(0)}|\mathbf{b},\boldsymbol{\rho}}(0|\mathbf{b},\boldsymbol{\rho})|\boldsymbol{\rho}\}\}; \tag{97}$$

$$E\{\rho_{ul}\rho_{vl}\hat{b}_u^{(0)}\hat{b}_v^{(0)}\} = E\{E\{E\{\rho_{ul}\rho_{vl}\hat{b}_u^{(0)}\hat{b}_v^{(0)}|\mathbf{b},\boldsymbol{\rho}\}|\boldsymbol{\rho}\}\}$$
$$= E\{E\{\rho_{ul}\rho_{vl}[16\rho_{uv}D_h^2\sigma_n^4 f_{\tilde{b}_u^{(0)},\tilde{b}_v^{(0)}|\mathbf{b},\boldsymbol{\rho}}(0,0|\mathbf{b},\boldsymbol{\rho})$$
$$+(2Q_u-1)(2Q_v-1)]|\boldsymbol{\rho}\}\}, \tag{98}$$

where

$$Q_l = Q\left(-\frac{E\{\tilde{b}_l^{(0)}|\mathbf{b},\boldsymbol{\rho}\}}{\sigma}\right), \tag{99}$$

where $\mathrm{Var}\{\zeta_l\} = 4D_h^2\sigma_n^4$ is the variance of the total background noise forming at the GR back end; σ_n^2 is the variance of the additive Gaussian noise at the PF and AF outputs of GR front end linear tract; $Q(x)$ is the Gaussian Q-function defined by (79).

Although numerical integration in [12, 17] can be adopted for determining the optimal PCF $p_{1,\mathrm{opt}}$ for the first stage based on (91)–(97), it requires a huge computational complexity. To simplify this problem, we assume that the total background noise forming at the GR back end can be considered as a constant factor and may be small enough such that the Q functions in (96) and (98) are all constants and (97) can be approximated by zero. That is

$$4D_h^2\sigma_n^4 \ll \min_{\{S_k,\boldsymbol{\rho}\}}\{M\{\tilde{b}_u^{(0)}|\mathbf{b},\boldsymbol{\rho}\}\}^2 = \frac{4S_m^2}{N^2}, \tag{100}$$

where [36]

$$S_m = \min S_k; \quad \sum_{k\neq m}^{K} S_k b_k \rho_{kl} = -S_m b_m \rho'_{ml}; \quad \text{and} \quad \min|\rho_{ml} - \rho'_{ml}| = 2N^{-1}. \tag{101}$$

Now, we can rewrite (96) and (98) in the following form:

$$E\{E\{\rho_{ul}\rho_{vl}\hat{b}_u^{(0)}(2Q_v-1)|\boldsymbol{\rho}\}\} = B_1 E\{\rho_{ul}\rho_{vl}\}E\{\hat{b}_u^{(0)}|\boldsymbol{\rho}\} = 0; \tag{102}$$

$$E\{E\{\rho_{ul}\rho_{vl}[16\rho_{uv}D_h^2\sigma_n^4 f_{\tilde{b}_u^{(0)},\tilde{b}_v^{(0)}|\mathbf{b},\boldsymbol{\rho}}(0,0|\mathbf{b},\boldsymbol{\rho}) + (2Q_u-1)(2Q_v-1)]|\boldsymbol{\rho}\}\}$$
$$= E\{E\{16D_h^2\sigma_n^4\rho_{ul}\rho_{vl}\rho_{uv}f_{\tilde{b}_u^{(0)},\tilde{b}_v^{(0)}|\mathbf{b},\boldsymbol{\rho}}(0,0|\mathbf{b},\boldsymbol{\rho})|\boldsymbol{\rho}\}\} + B_2 E\{E\{\rho_{ul}\rho_{vl}|\boldsymbol{\rho}\}\}$$
$$= E\{E\{16D_h^2\sigma_n^4\rho_{ul}\rho_{vl}\rho_{uv}f_{\tilde{b}_u^{(0)},\tilde{b}_v^{(0)}|\mathbf{b},\boldsymbol{\rho}}(0,0|\mathbf{b},\boldsymbol{\rho})|\boldsymbol{\rho}\}\}, \tag{103}$$

where B_1 and B_2 are constants. According to the assumptions made above, $f_{\tilde{b}_u^{(0)},\tilde{b}_v^{(0)}|\mathbf{b},\rho}(0,0|\mathbf{b},\rho)$ can be expressed by

$$f_{\tilde{b}_u^{(0)},\tilde{b}_v^{(0)}|\mathbf{b},\boldsymbol{\rho}}(0,0|\mathbf{b},\boldsymbol{\rho}) = \frac{\exp(-\frac{1}{2}\mathbf{m}_b^T\mathbf{B}_b^{-1}\mathbf{m}_b)}{8\pi D_h^2\sigma_n^4\sqrt{1-\rho_{uv}^2}}, \tag{104}$$

where $\mathbf{m}_b = \{E\{\tilde{b}_u^{(0)}|\mathbf{b},\boldsymbol{\rho}\}, E\{\tilde{b}_v^{(0)}|\mathbf{b},\boldsymbol{\rho}\}\}^T$ and $\mathbf{B}_b = E\{(\tilde{\mathbf{b}}-\mathbf{m}_b)(\tilde{\mathbf{b}}-\mathbf{m}_b)^T\}$ with $\tilde{\mathbf{b}} = [\tilde{b}_u^{(0)}, \tilde{b}_v^{(0)}]^T$.

Since $\mathbf{B}_b^{-1}$ is a positive semi-definite matrix, i.e., $\mathbf{m}_b^T\mathbf{B}_b^{-1}\mathbf{m}_b \geq 0$, we can have

$$0 < f_{\tilde{b}_u^{(0)},\tilde{b}_v^{(0)}|\mathbf{b},\boldsymbol{\rho}}(0,0|\mathbf{b},\boldsymbol{\rho}) \leq \max_{\substack{\rho_{uv}\\ \rho_{uv}\neq\pm1}} \frac{1}{8\pi D_h^2\sigma_n^4\sqrt{1-\rho_{uv}^2}}. \tag{105}$$

With the above results,

$$\min_{\rho_{uv},\rho_{uv}\neq\pm1}\sqrt{1-\rho_{uv}^2} = \frac{2\sqrt{N-1}}{N}, \tag{106}$$

where [36] $\rho_{uv} = 1-2N^{-1}$or $-1+2N^{-1}$ and

$$E\{\rho_{ul}\rho_{vl}\rho_{uv}\} = \sum_{m=1}^{N}\sum_{p=1}^{N}\sum_{q=1}^{N}E\{c_{um}c_{lm}c_{vp}c_{lp}c_{uq}c_{vq}\} = \sum_{m=1}^{N}\frac{1}{N^3} = \frac{1}{N^2} \tag{107}$$

we can derive a range of $p_{1,\text{opt}}$:

$$\frac{\sum_{u\neq l}^{K}S_u^2(1-2P_{\text{BER}_{e,u}})}{\sum_{u\neq l}^{K}S_u^2 + \frac{1}{\pi\sqrt{N-1}}\sum_{u\neq l}^{K}\sum_{v\neq l,u}^{K}S_uS_v} \leq p_{1,\text{opt}} < 1 - \frac{2\sum_{u\neq l}^{K}S_u^2P_{\text{BER}_{e,u}}}{\sum_{u\neq l}^{K}S_u^2}. \tag{108}$$

If the power control is perfect, i.e., $S_u = S_v = S$ and $P_{\text{BER}_{e,u}} = P_{\text{BER}_e}$, where P_{BER_e} is approximated by the BER of high SNR case, i.e., we have the $Q\left(\sqrt{\frac{N}{K-1}}\right)$ function [6, 29], (108) can be rewritten as

$$\frac{1-2Q\left(\sqrt{\frac{N}{K-1}}\right)}{1+\frac{K-2}{\pi\sqrt{N-1}}} \leq p_{1,\text{opt}} < 1-2Q\left(\sqrt{\frac{N}{K-1}}\right). \tag{109}$$

It is interesting to see that the lower and upper boundary values can be explicitly calculated from the processing gain N and the number of users K.

7 Simulation Results

7.1 FIR Beamforming and MIMO System

For a definition of numerical results using simulation, we consider the typical urban channel [16] of the GSM/EDGE system as a practical example. As is usually done for

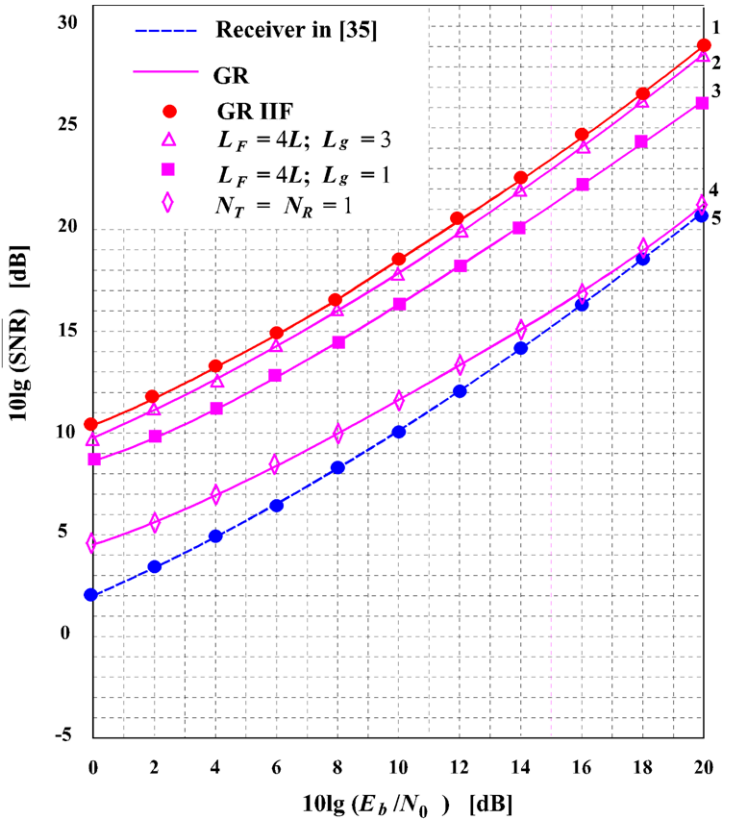

Fig. 3 Average SNR of MMSE linear equalization at the GR for beamforming with FIR and infinite impulse response filters. The result for single antenna transmission is also indicated (the curve 4). IIR is for infinite impulse response beamforming filter

GSM/EDGE, the transmit pulse shape is modeled as a linearized Gaussian minimum-shift keying pulse [37]. The GR input linear system filter is a square-root raised-cosine filter with roll-off factor 0.3. Furthermore, we assume $N_T = 3$ transmit and $N_R = 3$ receive antennas and a maximum channel length of $L = 5$. The correlation coefficient between all pairs of transmit antennas is $\rho = 0.5$.

Figure 3 shows the average $\overline{\text{SNR}}$ as a function of the SNR noted by $\frac{E_b}{N_0}$ for the GR with MMSE linear equalization in the cases of FIR (the curves 2 and 3) and infinite impulse response (the curve 1) beamforming filter, respectively, where E_b denotes the average received energy per symbol. Curve 5 corresponds to the case for infinite impulse response beamforming filter for receiver discussed in [38]. The $\overline{\text{SNR}}$ was obtained by averaging the respective SNRs over 1000 independent realizations of the typical urban channel. For this purpose, in the case of FIR beamforming filter at the GR, the SNR given by (39) was used and the corresponding beamforming filters at the GR were calculated using the gradient algorithm discussed in Sect. 3. For infinite impulse response beamforming filter at the GR the result given in [53] was used.

For comparison, we also show simulation results with FIR linear equalization filters at the GR of length $L_F = 4L$ for FIR beamforming filters at the GR with $L_g = 1$ (curve 3) optimized for infinite impulse response linear equalization filters at the GR. These simulation results confirm that sufficiently long FIR linear equalization filters at the GR closely approach the performance of infinite impulse response linear equalization filters at the GR, which are necessary for (58) to be valid. As expected, the beamforming with infinite impulse response beamforming filters at the GR constitutes a natural performance upper bound for the beamforming with FIR beamforming filters at the GR. However, interestingly, for the typical urban channel the FIR beamforming filter of length $L_g = 3$ (curve 2) is sufficient to closely approach the performance of the infinite impulse response beamforming at the GR (curve 1).

We note that for high values of $\frac{E_b}{N_0}$ even an FIR beamforming filter at the GR of length $L_g = 1$ achieves a performance gain of more than 4.5 dB compared to single antenna transmission, i.e., $N_T = N_R = 1$ (curve 4). Additional simulations not shown here for other GSM/EDGE channel profiles have shown that, in general, the FIR beamforming filter at the GR of length $L_g \leq 6$ is sufficient to closely approach the performance of the infinite impulse response beamforming at the GR. Thereby, the value of L_g required to approach the performance of the infinite impulse response beamforming at the GR seems to be smaller if the channel is less frequency selective.

7.2 Channel Estimation and Spatially Correlation

We choose the 0.5 rate Low Density Parity Check (LDPC) code with a block length of 64 800 bits, which is also adopted by DVB-S.2 standard [13]. QPSK modulation with Gray mapping is adopted in $N_T = N_R = 4$ MIMO system. Meanwhile, we set $\sigma^2_{\Delta h} = 1, N_T = N_R$, and $E_P = E_b$. The channel is generated with coherence time of $N_P + N_D = 85$ MIMO vector symbol intervals, and then a LDPC codeword is transmitted via 100 channel coherent time intervals for QPSK modulation. For GR spatially correlated MIMO channel the GR array correlation matrix $\mathbf{R_r}$ with the following elements is adopted [31]: $\mathbf{R_r}(n,n) = 1$, $\mathbf{R_r}(m,n) = \mathbf{R_r^*}(m,n)$, $m,n = 1,2,3,4$; $\mathbf{R_r}(1,2) = \mathbf{R_r}(2,3) = \mathbf{R_r}(3,4) = 0.4290 + 0.7766j$; $\mathbf{R_r}(1,3) = \mathbf{R_r}(2,4) = -0.3642 + 0.5490j$; and $\mathbf{R_r}(1,4) = -0.4527 - 0.0015j$.

The performance comparison, in terms of BER, of the proposed soft-output MMSE GR, the modified soft-output MMSE GR [51], the conventional soft-output MMSE GR [55], and the conventional MMSE GR [24] is presented in Fig. 4 for spatially independent MIMO channel and GR receiver spatially correlated MIMO channel. Also, a comparison with the soft-output MMSE V-BLAST detector discussed in [26] is made. The proposed MMSE GR outperforms all the existing schemes with considerable gain, especially for receiver correlation MIMO channel scenario. The underlying reason of this improvement is that the MMSE GR, by taking channel estimation error, decision error propagation and channel correlation into account, can output more reliable LLR to the channel decoder. As the channel estimation error is the dominant factor influencing the system performance under the lower SNR region, it can be observed that the BER of the conventional soft-output MMSE GR [55] is slightly better than that of the modified soft-output MMSE GR in the case of spatially independent MIMO channel.

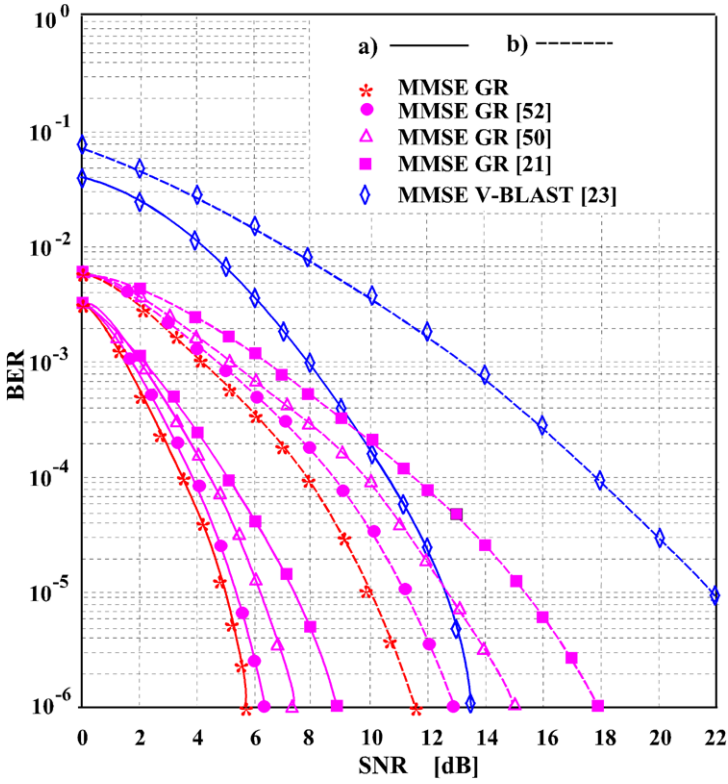

Fig. 4 BER performance of different detectors under (**a**) spatially independent MIMO channel and (**b**) receiver spatially correlated MIMO channel

7.3 Hybrid Selection/Maximal-Ratio Combining

In this subsection we discuss some examples of the GR performance under quadrature subbranch HS/MRC and HS/MRC schemes and compare with the conventional HS/MRC receiver. The average SER of coherent BPSK and 8-PAM signals under processing by the GR with quadrature subbranch HS/MRC and HS/MRC schemes as a function of the average SNR per symbol per diversity branch for various values of $2L$ and $2N = 8$ is presented in Fig. 5. It is seen that the GR performance with quadrature subbranch HS/MRC and HS/MRC schemes with $(L, N) = (3, 4)$ achieves virtually the same performance as the GR with traditional MRC, and that the performance with $(L, N) = (2, 4)$ is typically less than 0.5 dB in SNR poorer than the GR with traditional MRC in [21]. Also, a comparison with the traditional HS/MRC receiver is made. The advantage of GR employment is evident.

The average SER of coherent BPSK and 8-PAM signals under processing by the GR with quadrature subbranch HS/MRC and HS/MRC schemes as a function of av-

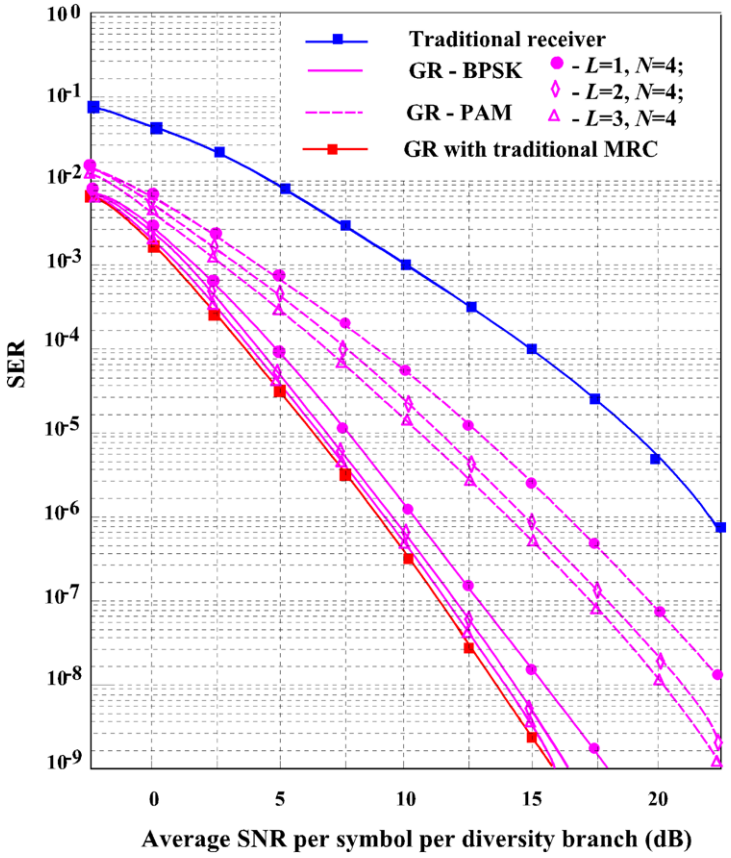

Fig. 5 Average SER of coherent BPSK and 8-PAM for the GR under quadrature subbranch HS/MRC and HS/MRC schemes versus the average SNR per symbol per diversity for various values of $2L$ with $2N = 8$

erage SNR per symbol per diversity branch for various values of $2N$ with $2L = 4$ is shown in Fig. 6. We note the substantial benefits of increasing the number of diversity branches N for fixed L. Comparison with the traditional HS/MRC receiver is made. The advantage of GR employment is evident.

Comparative analysis of the average BER as a function of the average SNR per bit per diversity branch of coherent BPSK signals under the use of the GR with quadrature subbranch HS/MRC and HS/MRC schemes and the GR with traditional HS/MRC scheme for various values of L with $N = 4$ is presented in Fig. 7. To achieve the same value of average SNR per bit per diversity branch, we should choose $2L$ quadrature branches for the GR with quadrature subbranch HS/MRC and HS/MRC schemes and L diversity branches for the GR with traditional HS/MRC scheme. Figure 7 shows that the performance of the GR with quadrature subbranch HS/MRC and HS/MRC schemes is much better than that of the GR with traditional HS/MRC scheme, about 0.5 dB to 1.2 dB when L is less than one half N. This difference decreases with increasing L. This is expected because, when $L = N$, we obtain the

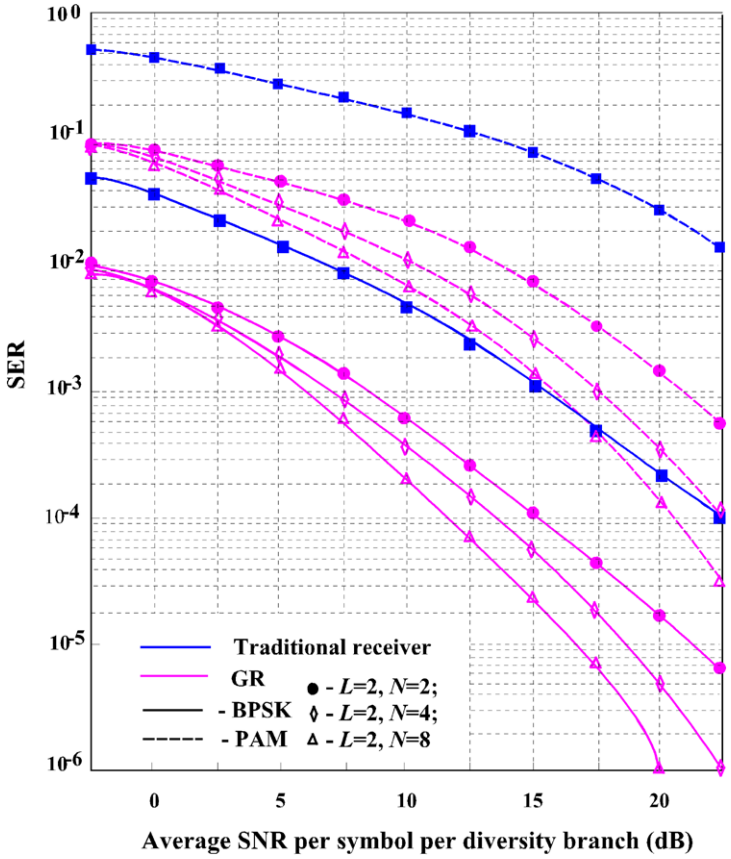

Fig. 6 Average SER of coherent BPSK and 8-PAM for the GR under quadrature subbranch HS/MRC and HS/MRC versus the average SNR per symbol per diversity for various values of $2N$ with $2L = 4$

same performance. Some discussion of the increases in GR complexity and power consumption is in order.

We first note that the GR with quadrature subbranch HS/MRC and HS/MRC schemes requires the same number of antennas as the GR with traditional HS/MRC scheme. On the other hand, the former requires twice as many comparators as the latter, to select the best signals for further processing. However, the GR designs that process the quadrature signal components will require $2L$ receiver chains for either the GR with quadrature subbranch HS/MRC and HS/MRC schemes or the GR with traditional HS/MRC scheme. Such receiver designs will use only a little additional power, as the GR chains consume much more power than the comparators.

On the other hand, the GR designs that implement co-phasing of the branch signals without splitting the branch signals into the quadrature components will require L receiver chains for the GR with traditional HS/MRC scheme and $2L$ receiver chains for the GR with quadrature subbranch HS/MRC and HS/MRC schemes, with corresponding hardware and power consumption increases.

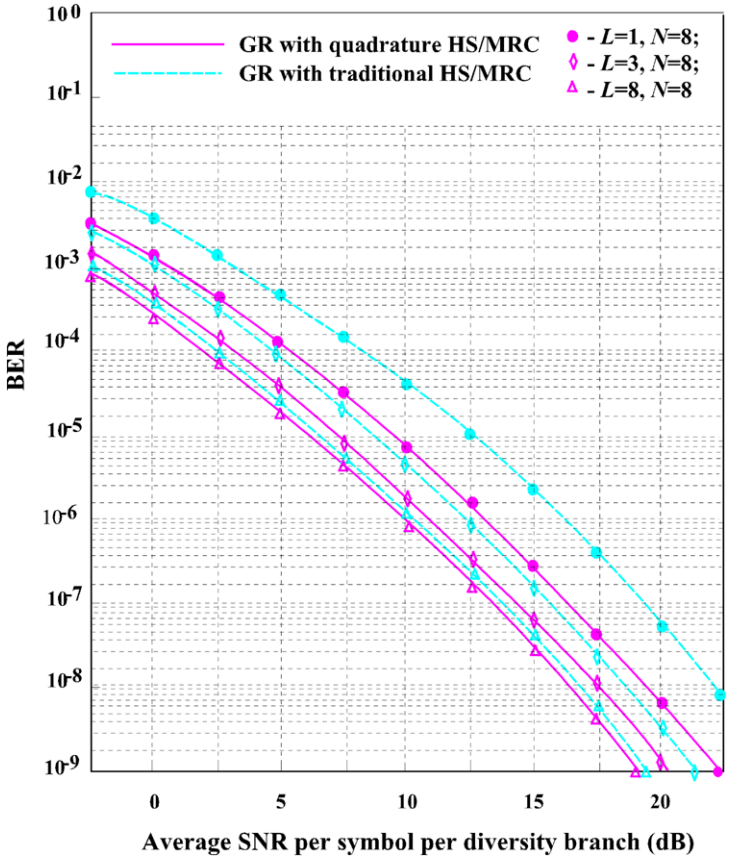

Fig. 7 Comparison of the average BER of coherent BPSK and 8-PAM for the GR under quadrature subbranch HS/MRC and HS/MRC schemes for various values of $2L$ with $N = 8$

7.4 Synchronous DS-CDMA System

To demonstrate the usefulness of range of the optimal PCF given by (108), we performed a number of simulations for a synchronous DS-CDMA wireless communication system employing GR with perfect power control. In the simulations, random spreading codes with length $N = 64$ were used for each user and the number of users was $K = 40$ [50]. Figure 8 shows the BER performance of the single-stage hard-decision GR based on the PPIC for different magnitudes of SNR and various values of PCFs, where the optimal PCF for the first stage lies between 0.3169 (lower boundary) and 0.7998 (upper boundary). It can be seen that, for all the SNR cases, the GR based on the PPIC using the average of the lower and upper boundary values, i.e., 0.5584, as the PCF, has a BER performance close to that using the optimal PCF. Also, comparative results when the GR is employed by DS-CDMA wireless communication systems with the conventional detector discussed in [40] are presented. These

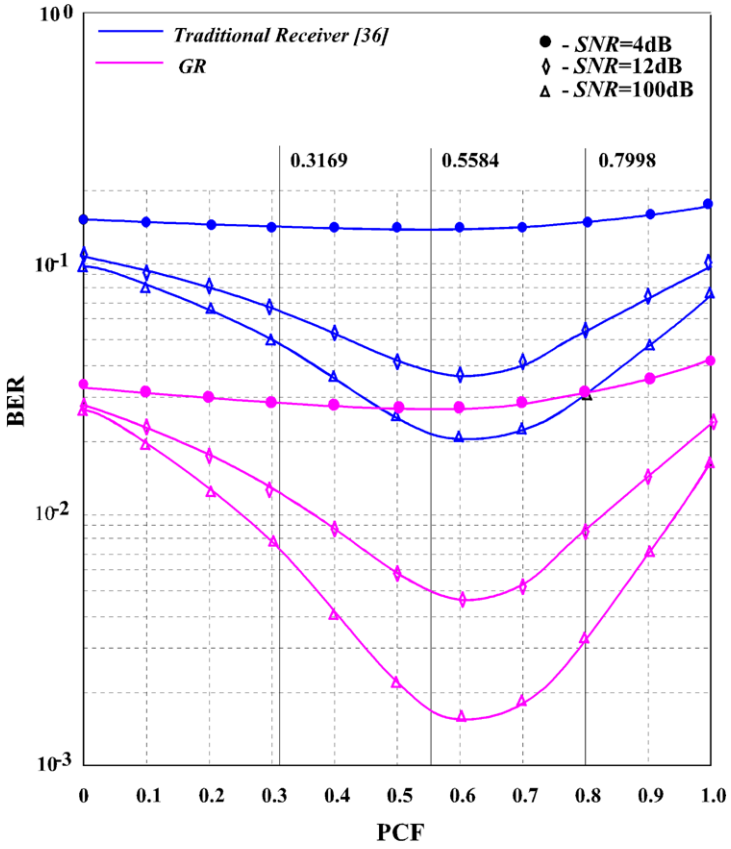

Fig. 8 The BER performance of the single-stage GR based on the PPIC with hard decisions for different SNRs and PCFs

results show us the great superiority of the GR employment in DS-CDMA wireless communication systems in comparison with employment of the conventional detector discussed in [40].

Figure 9 shows the BER performance at each stage for the three-stage GR based on the PPIC using different PCFs at the first stage, i.e., the average value and an arbitrary value. The PCFs for these two three-stages cases are $(a_1, a_2, a_3) = 0.5584; 0.8; 0.9$ and $(a_1, a_2, a_3) = 0.7; 0.8; 0.9$, respectively. The results demonstrate that the BER performance of the GR employed by DS-CDMA wireless communication systems of the cases using the PCF at the first stage is better than the BER performance of the GR implemented in DS-CDMA wireless communication system using an arbitrary PCF at the first stage. Furthermore, the BER performance of the GR at the second stage for the case of PCF at the first stage achieves a GR BER performance comparable to that of the three-stage GR based on PPIC using an arbitrary PCF at the first stage.

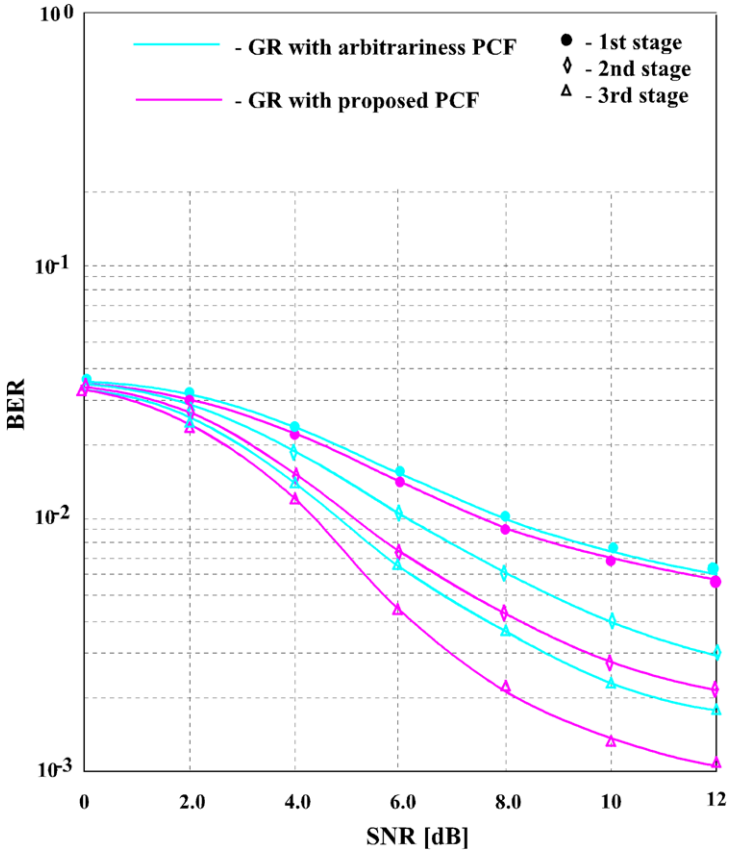

Fig. 9 The BER performance at each stage for three-stage GR based on the PPIC with hard decisions for different PCFs at the first stage, i.e. an average value and an arbitrary value

8 Conclusions

In this paper, we have considered the FIR beamforming at the GR with perfect channel state information for single carrier transmission over frequency-selective fading channels with zero-forcing linear equalization and GR MMSE linear equalization. We employed a gradient algorithm for efficient recursive calculation of the FIR beamforming filters at the GR. Our results show that for typical GSM/EDGE channel profiles short FIR beamforming filters at the GR suffice to closely approach the performance of optimum infinite impulse response beamforming at the GR discussed in [53]. This is a significant result, since in practice, the quantized beamforming filter coefficients have to be fed back from the receiver to the transmitter, which makes short beamforming filters preferable.

The proposed MMSE GR outperforms all the existing schemes with considerable gain especially for receiver correlation MIMO channel scenario. The underlying reason of this improvement is that the MMSE GR, by taking the channel estimation error, decision error propagation, and channel correlation into account, can output more re-

liable LLR to channel decoder. As channel estimation error is the dominant factor influencing the system performance under lower SNR region, it can observed that the BER of the conventional soft-output MMSE GR [55] is slightly better than that of the modified soft-output MMSE GR in the case of spatially independent MIMO channel.

The performance of the GR with quadrature subbranch HS/MRC and HS/MRC schemes for 1-D signal modulations in Rayleigh fading is investigated. The SER of M-ary PAM, including coherent BPSK, QPSK, and M-ary QAM modulation, is derived. Results show that the GR with quadrature subbranch HS/MRC and HS/MRC schemes performs substantially better than the GR with traditional HS/MRC scheme, particularly, when L is smaller than one half N, and much better than the traditional HS/MRC receiver.

We have also derived a range of the optimal PCF for the GR first stage based on the PPIC, which is employed by a DS-CDMA wireless communication system, with hard decisions in AWGN environment. Computer simulation results have shown that the BER performance of the GR employed by DS-CDMA wireless communication systems of the case using the average of the lower and upper boundary values is close to the BER performance of the GR of the case using the real optimal PCF, whether the SNR is high or low.

It has also been shown that the GR employment in DS-CDMA wireless communication system allows us to observe a great superiority over the conventional detector. It has also been demonstrated that the two-stage GR based on the PPIC using the PCF at the first stage achieves a GR BER performance comparable to that of the three-stage GR based on the PPIC using an arbitrary PCF at the first stage. This means that under the same BER performance, the number of stages (or complexity) required for the multistage GR based on the PPIC can be reduced when the PCF is used at the first stage. As well as AWGN environments, it can be shown that the PCF selection approach is applicable to multipath fading cases under GR employment in DS-CDMA wireless communication systems even if non-perfect power control is assumed.

Acknowledgements This work was supported by Kyungpook National University Research Grant, 2009. Additionally, the author would like to thank the anonymous reviewers for the comments and suggestions that helped to improve the quality of this paper.

References

1. K. Abed-Meraim, W. Qaiu, Y. Hua, Blind system identification. Proc. IEEE **85**(8), 1310–1322 (1997)
2. M.-S. Alouini, A.J. Goldsmith, A unified approach for calculating error rates of linearly modulated signals over generalized fading channels. IEEE Trans. Commun. **47**(9), 1324–1334 (1999)
3. M.-S. Alouini, M.K. Simon, Performance of coherent receivers with hybrid SC/MRC over Nakagami m-fading channels. IEEE Trans. Veh. Technol. **48**(4), 1155–1164 (1999)
4. M.-S. Alouini, M.K. Simon, An MGF-based on performance analysis of generalized selection combining over Rayleigh fading channels. IEEE Trans. Commun. **48**(3), 401–415 (2000)
5. A. Annamalai, C. Tellambura, A new approach to performance evaluation of generalized selection diversity receivers in wireless channels, in *Proc. IEEE Vehicle Technology Conference*, vol. 4 (2001), pp. 2309–2313
6. D.R. Brown III, C.R. Johnson Jr., SINR, power efficiency, and theoretical system capacity of parallel interference cancellation. J. Commun. Netw. **3**(9), 228–237 (2001)
7. J. Choi, R. Heath, Interpolation based transmit beamforming for MIMO-OFDM with limited feedback. IEEE Trans. Signal Process. **53**(11), 4125–4135 (2005)

8. J.M. Cioffi, G.P. Dudevoir, M.V. Eyuboglu, G.D. Forney Jr., MMSE decision-feedback equalizers and coding—part I: equalization results. IEEE Trans. Commun. **43**(10), 2582–2594 (1995)
9. M.V. Clark, L.J. Greenstein, W.K. Kennedy, M. Shafi, Optimum linear diversity receivers for mobile communications. IEEE Trans. Veh. Technol. **43**(2), 47–56 (1994)
10. J.W. Craig, A new, simple and exact result for calculating the probability of error for two-dimensional signal constellations, in *Proc. IEEE International Conference on Military Communications, Milcom'91* (1991), pp. 571–575
11. P. Dighe, R. Mallik, S. Jamuar, Analysis of transmit-receive diversity in Rayleigh fading. IEEE Trans. Commun. **51**(4), 694–703 (2003)
12. D. Divsalar, M.K. Simon, D. Raphaeli, Improved parallel interference cancellation for CDMA. IEEE Trans. Commun. **46**(2), 258–268 (1998)
13. ETSI EN302 307 V1.1.1 (2004–2006), Digital video broadcasting (DVB); Second generation framing structure, channel coding and modulation systems for broadcasting, interactive services, news gathering and other broad-band satellite applications
14. W. Gerstacker, R. Schober, Equalization concepts for EDGE. IEEE Trans. Wirel. Commun. **1**(1), 190–199 (2002)
15. M. Ghotobi, M.R. Soleymani, Multiuser detection of DS-CDMA signals using partial parallel interference cancellation in satellite communications. IEEE J. Sel. Areas Commun. **22**(4), 584–593 (2004)
16. GSM recommendation 05.05: Propagation conditions, Version 5.3.0, release 1996
17. D. Guo, Linear parallel interference cancellation in CDMA. M. Eng. thesis, Nat. Univ. Singapore, 1998
18. Y.-T. Hsieh, W.-R. Wu, Optimal two-stage decoupled partial PIC receivers for multiuser detection. IEEE Trans. Wirel. Commun. **4**(1), 112–127 (2005)
19. G. Jongren, M. Skoglund, B. Ottersten, Combining beamforming and orthogonal space-time block coding. IEEE Trans. Inf. Theory **48**(3), 611–627 (2002)
20. S.M. Kay, *Fundamentals of Statistical Signal Processing: Estimation Theory* (Prentice-Hall, Englewood Cliffs, 1993)
21. J.H. Kim, J.-H. Kim, V. Tuzlukov, W.-S. Yoon, Y.D. Kim, FFH and MCFH spread spectrum wireless sensor network systems based on the generalized approach to signal processing. WSEAS Trans. Comput. **3**(6), 1794–1801 (2004)
22. J.H. Kim, V. Tuzlukov, W.S. Yoon, Y.D. Kim, Generalized detector under nonorthogonal multipulse modulation in remote sensing systems. WSEAS Trans. Signal Process. **2**(1), 203–208 (2005)
23. J.H. Kim, V. Tuzlukov, W.S. Yoon, Y.D. Kim, Macrodiversity in wireless sensor networks based on the generalized approach to signal processing. WSEAS Trans. Commun. **4**(8), 648–653 (2005)
24. J.H. Kim, V. Tuzlukov, W.S. Yoon, Y.D. Kim, Performance analysis under multiple antennas in wireless sensor networks based on the generalized approach to signal processing. WSEAS Trans. Commun. **4**(7), 391–395 (2005)
25. N. Kong, L.B. Milstein, Average SNR of a generalized diversity selection combining scheme. IEEE Commun. Lett. **3**(3), 57–59 (1999)
26. K. Lee, J. Chun, Symbol detection in V-BLAST architectures under channel estimation error. IEEE Trans. Wirel. Commun. **6**(2), 593–597 (2007)
27. H. Lee, I. Lee, New approach for error compensation in coded V-BLAST OFDM systems. IEEE Trans. Commun. **55**(2), 345–355 (2007)
28. H. Lee, B. Lee, I. Lee, Iterative detection and decoding with an improved V-BLAST for MIMO-OFDM systems. IEEE J. Sel. Areas Commun. **24**(3), 504–513 (2006)
29. J.C. Liberti Jr., T.S. Rappaport, *Smart Antennas for Wireless Communications: IS-95 and Third Generation CDMA Applications* (Prentice Hall, Upper Saddle River, 1999)
30. D. Love, R. Heath, T. Strohmer, Grassmannian beamforming for multiple-input multiple-output wireless systems. IEEE Trans. Inf. Theory **49**(10), 2735–2747 (2003)
31. Lucent, Nokia, Simens, Ericsson, A standard set of MIMO radio propagation channels, 3GPP TSGR323 R1-01-1179
32. R.K. Malik, M.Z. Win, Analysis of hybrid selection/maximal-ratio combining in correlated Nakagami fading. IEEE Trans. Commun. **50**(8), 1372–1383 (2002)
33. T.L. Marzetta, BLAST training: estimating channel characteristics for high-capacity space-time wireless, in *Proc. 37th Annual Allerton Conference on Communications, Control, and Computing* (1999), pp. 958–966
34. U. Mengali, A.N.D. Andrea, *Synchronization Techniques for Digital Receivers* (Plenum, New York, 1997)

35. T.K. Moon, W.C. Stirling, *Mathematical Methods and Algorithms for Signal Processing* (Prentice Hall, New York, 2000)
36. R.K. Morrow Jr., J.S. Lehnert, Bit-to-bit error dependence in slotted DS/SSMA packer systems with random signature sequences. IEEE Trans. Commun. **37**(10), 1052–1061 (1989)
37. K. Mukkavilli, A. Sabharwal, E. Erkip, B. Aazhang, Beamforming with finite rate feedback in multiple antenna systems. IEEE Trans. Inf. Theory **49**(10), 2562–2579 (2003)
38. D.P. Palomar, M.A. Lagunas, Joint transmit-receive space-time equalization in spatially correlated MIMO channels: a beamforming approach. IEEE J. Sel. Areas Commun. **21**, 730–743 (2003)
39. A. Papoulis, S.U. Pillai, *Probability, Random Variables and Stochastic Processes*, 4th edn. (McGraw-Hill, New York, 2002)
40. J.G. Proakis, *Digital Communications*, 4th edn. (McGraw-Hill, New York, 2001)
41. P.G. Renucci, B.D. Woerner, Optimization of soft interference cancellation for DS-CDMA. Electron. Lett. **34**(4), 731–733 (1998)
42. G. Taricco, E. Biglieri, Space-time decoding with imperfect channel estimation. IEEE Trans. Wirel. Commun. **4**(4), 1874–1888 (2005)
43. L. Tong, S. Perreau, Multichannel blind identification: from subspace to maximal likelihood methods. Proc. IEEE **86**(10), 1951–1968 (1998)
44. J.K. Tugnait, L. Tong, Z. Ding, Single user channel estimation and equalization. IEEE Signal Process. Mag. **17**(3), 17–28 (2000)
45. V. Tuzlukov, *Signal Processing in Noise: A New Methodology* (IEC, Minsk, 1998)
46. V. Tuzlukov, A new approach to signal detection theory. Digit. Signal Process., Rev. J. **8**(3), 166–184 (1998)
47. V. Tuzlukov, *Signal Detection Theory* (Springer, New York, 2001)
48. V. Tuzlukov, *Signal Processing Noise* (CRC Press, Boca Raton, 2002)
49. V. Tuzlukov, *Signal and Image Processing in Navigational Systems* (CRC Press, Boca Raton, 2004)
50. V. Tuzlukov, Selection of partial cancellation factors in DS-CDMA systems employing the generalized detector, in *Proc.12th WSEAS International Conference on Communications: New Aspects of Communications* (2008), pp. 129–134
51. V. Tuzlukov, Multiuser generalized detector for uniformly quantized synchronous CDMA signals in wireless sensor networks with additive white Gaussian noise channels, in *Proc. International Conference on Control, Automation, and Systems, ICCAS 2008* (2008), pp. 1526–1531
52. V. Tuzlukov, Multiuser generalized detector for uniformly quantized synchronous CDMA signals in AWGN Channels. Telecommun. Rev. **20**(5), 836–848 (2010)
53. V. Tuzlukov, W.S. Yoon, Y.D. Kim, Adaptive beam-former generalized detector in wireless sensor networks, in *Proc. The IASTED International Conference on Parallel and Distributed Computing and Networks, PDCN 2004* (2004), pp. 195–200
54. V. Tuzlukov, W.S. Yoon, Y.D. Kim, Wireless sensor networks based on the generalized approach to signal processing with fading channels and receive antenna array. WSEAS Trans. Circuits Syst. **10**(3), 2149–2155 (2004)
55. V. Tuzlukov, W.S. Yoon, Y.D. Kim, MMSE multiuser generalized detector for nonorthogonal multipulse modulation in wireless sensor networks, in *Proc. 9th World Multi-Conference on Systemics, Cybernetics and Informatics, WMSCI 2005* (2005)
56. J. Wang, S. Li, Capacity and performance of MIMO BICM system with soft-output MMSE soft interference cancellation, in *Proc. CCNC 2008* (2008)
57. M.X. Win, J.H. Winters, Analysis of hybrid selection/maximal ratio combining in Rayleigh fading. IEEE Trans. Commun. **47**(12), 1773–1776 (1999)
58. M.Z. Win, J.H. Winters, Virtual branch analysis of symbol error probability for hybrid selection/maximal-ratio combining in Rayleigh fading. IEEE Trans. Commun. **49**(11), 1926–1934 (2001)
59. K.-M. Wu, C.-L. Wang, Soft-input soft-output partial parallel interference cancellation for DS-CDMA systems, in *Proc. IEEE International Conference on Communications, ICC'01* (2001), pp. 1172–1176
60. G. Xue, J.F. Weng, T. Le-Ngoc, S. Tahar, An analytic model for performance evaluation of parallel interference cancellers in CDMA systems. IEEE Commun. Lett. **4**(6), 184–186 (2000)
61. R.E. Ziemer, W.H. Tranter, *Principles of Communications: Systems, Modulation, and Noise*, 6th edn. (Wiley, New York, 2010)